Advanced Control of Grid-Connected Microgrids: Challenges, Advances, and Trends

Oluleke Babayomi, *Senior Member, IEEE*, Yu Li, *Member, IEEE*, Zhenbin Zhang, *Senior Member, IEEE*, and Ki-Bum Park, *Member, IEEE*

***Abstract*—Sustainable microgrids are powered by renewable energy sources [e.g., solar photovoltaic (PV) and wind energy], and these support the reliability, resilience, and the decarbonization of the electrical grid. In recent decades, advanced nonlinear control techniques are increasingly being used to integrate power converters to meet grid requirements. This study reviews the advanced nonlinear control techniques predominantly used for grid-connected converters, namely, data-driven control, nonlinear model predictive control, direct power control, sliding mode control, disturbance-observer methods, and passivity control. Recent advances in these control policies are highlighted and various design and performance features are compared. Solutions for grid-synchronization stability, nonideal and distorted grid conditions, circulating current suppression, power quality, harmonics suppression, and grid support are presented—as well as the future trends of the advanced control methods. The study indicates that advanced control offers advantages in dynamic performance, disturbance rejection and multiobjective control over linear control for multiobjective and multitimescale microgrids.**

***Index Terms*—Artificial intelligence, data-driven control, disturbance observer, grid-connected converters, microgrids, model predictive control (MPC), passivity, power converters, sliding mode.**

Nomenclature

ANFIS	Adaptive neuro-fuzzy inference system.
ANN	Artificial neural network.
CCS-MPC	Continuous control-set MPC.
DNN	Deep neural network.
DOBC	Disturbance-observer-based control.
DFIG	Dual-fed induction generator.
DPC	Direct power control.
ESS	Energy storage system.

Received 27 July 2024; revised 18 October 2024; accepted 28 December 2024. Date of publication 6 January 2025; date of current version 20 March 2025. This work was supported in part by the Korea Institute of Energy Technology Evaluation and Planning (KETEP), in part by the Korea Government (MOTIE) under Grant 20225000000100, and in part by the National Natural Science Foundation of China under Grant 52277191 and Grant 52277192. Recommended for publication by Associate Editor F. D. Freijedo. *(Corresponding authors: Ki-Bum Park; Zhenbin Zhang.)*

Oluleke Babayomi and Ki-Bum Park are with the Cho Chun Shik Graduate School of Mobility, Korea Advanced Institute of Science and Technology, Daejeon 34051, South Korea (e-mail: babayomi@ieee.org; ki-bum.park@kaist.ac.kr).

Yu Li is with the Laser Institute, Qilu University of Technology (Shandong Academy of Sciences), Jinan 250104, China (e-mail: liyu@sdlaser.cn).

Zhenbin Zhang is with the School of Electrical Engineering, Shandong University, Jinan 250061, China (e-mail: zbz@sdu.edu.cn).

Color versions of one or more figures in this article are available at https://doi.org/10.1109/TPEL.2025.3526246.

Digital Object Identifier 10.1109/TPEL.2025.3526246

I. Introduction

RENEWABLE-POWERED microgrids are essential technologies to decarbonize the electrical power grid and ensure environmental sustainability. These sustainable microgrids also support the grid's reliability and resilience. The renewable energy sources (RES) in grid-connected microgrids—especially solar photovoltaic (PV), wind energy, and energy storage—balance the demand for grid power, and provide support for a reliable grid. Also, the modularity and scalability of microgrids, and their adaptability for islanded operations guarantee uninterrupted power supply to critical load centers during grid downtime caused by high-impact, low-probability events like natural disasters. The integration of RES with the grid through microgrids is facilitated by (non)linear-controlled power electronic converters.

Linear controllers have linear schemes and require the linear model of the plant, e.g., proportional–integral, resonant, repetitive, and linear quadratic regulator controllers. When the plant is nonlinear, its linear model around an operating point is utilized. Systems that are maintained at nominal operating conditions and are subject to small disturbances can be controlled effectively with linear controllers [1]. However, grid-connected RES in microgrids experience a wide range of operational conditions and exogenous disturbances including load changes, intermittency of RES, grid-voltage perturbations, and age-related or dynamic temperature-induced model parameter uncertainties. Thus, they would benefit immensely from control methods that support nonlinear models and are stable over a wide region of operation.

Advanced nonlinear control techniques for power converters overcome the limitations of linear methods because they are capable of dealing with the nonlinearities in power electronic systems and increase the range of operational performance (that is not restricted to the nearby vicinity of an operating point) [2]. Furthermore, the stringent grid requirements of modern distributed RES can be met using advanced nonlinear control, without excessively increasing the complexity of the control scheme.

In the past two decades, advanced control techniques have grown in popularity among the research community; more than 90% of this growth occurred in the past decade (see Fig. 1). This development coincides with the availability of high-speed digital signal processors and field programmable gate arrays that accommodate the higher computational demands of several advanced control methods. These affordable hardware are increasingly utilized in academic institutions, increasing the

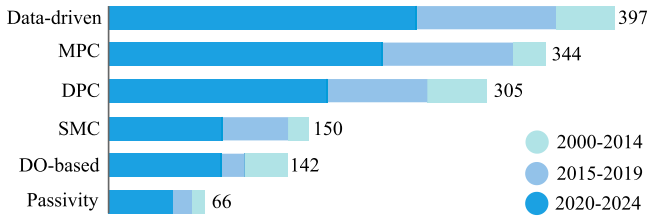

Fig. 1. Trend of publications on advanced control of grid-connected power converters (IEEE *Xplore* journal and magazine data accessed June 2024), where MPC is model predictive control, DPC is direct power control, SMC is sliding mode control, and DO is disturbance-observer-based control.

trained workforce and technical support community. Furthermore, industry interest too has been growing as the combined technical and market potentials of advanced methods, such as DOBC [3] and predictive control [4], have been demonstrated.

This study focuses on six leading control techniques for grid-connected microgrids, which altogether account for more than 92% of related published literature (in journals and magazines indexed by IEEE *Xplore*) over the past five years. These include data-driven control, nonlinear model predictive control (MPC), DPC, sliding mode control (SMC), DOBC, and passivity-based control (PBC). Other control methods include virtual oscillator [5], synergetic [6], internal model, hysteresis, feedback linearization, backstepping, and H_∞ control.

Data-driven control encompasses several techniques for controlling physical systems without dependence on a dynamic model. MPC is a multiobjective receding horizon scheme that seeks an optimal control-input sequence to optimize control objectives according to the system's constraints [7]. In this article, references to MPC refer specifically to *nonlinear MPC*. DPC applies the instantaneous power theory to directly control the active power and reactive power of pulsewidth modulated converters; it classically has no separate pulsewidth modulation (PWM) block or coordinate transformation [8]. SMC ensures that the control input is manipulated to make the state variables reach and remain on the sliding surface [9]. DOBC techniques provide two-degrees of freedom of control—for feedback control and disturbance rejection—by estimating the disturbances in the system, and compensating for them to either eliminate or attenuate their impact [10]. Passivity techniques allow to design controllers that ensure stability by satisfying decentralized stability conditions, and are scalable [11], [12], [13]. In this article, these methods will generally be referred to as *advanced control* techniques.

In prior studies, the control methods for voltage source converters (VSCs) in distributed generation [2] and microgrids [14] were reviewed. However, the control challenges of grid-connected VSCs and related research advances were not reported. Artificial intelligence control of microgrids was investigated in [15]. A cursory discussion of the principles of advanced control of power electronics in general was reported by Wu and Blaabjerg [16]. Nonetheless, these studies do not report on advances relating to the unique control challenges of grid-connected DERs or microgrids. Also, these prior studies all lack discussions on the future trends of research on the advanced control of grid-connected microgrids. In summary, the above literature are still yet to answer these questions. 1) What are the recent trends advanced control of grid-connected microgrid converters? 2) What are the motivations for advanced control of microgrids? 3) What are the relative differences in design requirements, complexity and performance of leading advanced control techniques for the grid-integration of DERs in microgrids?

In order to cover this research gap, the main contributions of this study include a systematic review of the leading advanced nonlinear control methods for RES grid-connected power converters in microgrids. Their relative advantages and disadvantages are compared in terms of computational burden, switching frequency, complexity, robustness, dynamic performance, disturbance rejection, and multiobjective control. Also, the first-known review (to the best of the authors' knowledge) on the data-driven control of grid-connected VSCs in microgrids is presented. Recent solutions to the challenges of advanced control are thoroughly discussed. Finally, the future trends are discussed. This article focuses on advanced *nonlinear* control methods, in contrast to advanced *linear* control reported in other studies [17].

The rest of this article is organized as follows. Section II presents the grid-integration requirements and control challenges of RES, and Section III reviews grid-synchronization stability criteria and solutions. Section IV clarifies the motivation for advanced hierarchical control of microgrids. Section V introduces the fundamental principles of the reviewed advanced control techniques, and Sections VI–VIII discuss the advances of the methods, their challenges and solutions. Section IX summarizes the characteristics of the techniques and their future trends. Finally, Section X concludes this article.

II. Control Requirements, Challenges, and Control Structures for Grid-Connected RES

In this section, the requirements, control challenges and control structures of grid-integrated RES will be discussed. Fig. 2 shows a typical grid-connected system comprising hybrid RES (solar PV and wind), and ESS. The RES-side system comprises RES and ESS along with their converters. The grid-side system comprises the grid-side converter (with its filter), microgrid and main grid. Coordinated control of multiple units can be facilitated by a communication network (where necessary).

A. Grid-Side Integration Requirements

The interconnection and grid integration requirements for RES have been evolving over the years, as the penetration of converter-interfaced RES increases. Since these RES are decoupled from the grid, special design and control requirements are implemented for identical grid support as classical synchronous generators. The grid codes, which vary among countries, are implemented to unify the power quality of electrical energy fed into the grid. Also, these grid codes also ensure that the distributed RES provide a measure of grid support to ensure grid stability during faults or and other perturbations from external disturbances.

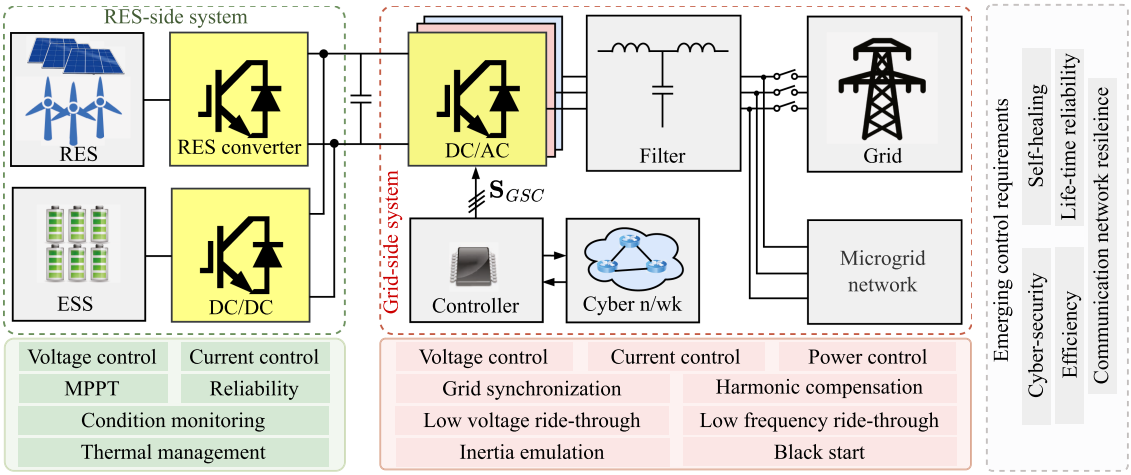

Fig. 2. Grid-connected RES in microgrids and their control requirements/objectives.

During normal operation, according to IEEE Std. 519–2014, RES (with PCC voltage from 120 V to 69 kV), are required to feed the grid with current at good power quality–generally with at most 4% total harmonic distortion (THD). This requirement aligns with IEC 61727 requirements for solar PV systems rated less than 10 kVA [18].

However, during abnormal grid conditions (grid faults), RES are required to continue to operate and support the grid for a minimum prespecified duration. The duration of (voltage and frequency) ride-through operation varies for different grid-codes. IEEE Std. 1547–2018 mandates continuous low-voltage ride-through (LVRT) within $90\% - 110\%$ of the nominal voltage [19]. At national levels, different countries delineate LVRT limits for wind, and PV systems. Furthermore, IEEE Std. 1547–2018 specifies how the RES are also required to provide grid support during the time they remain on by injecting reactive power for voltage stability and active power for frequency support. The afore-discussed RES grid-integration requirements, summarized in Fig. 2 lead to control challenges outlined in the following.

B. Control Challenges of Grid-Connected VSCs

The control challenges associated with the grid-side requirements, illustrated in Fig. 2, are discussed in this section.

1) Voltage, Current, and Power Control: The most fundamental control objective of the grid-tied VSC is to regulate the flow of electrical energy to/from the grid. This is classically achieved in grid-following VSCs by current control or DPC with respect to appropriate references. The former can ensure high quality current regulation, while the latter directly regulates the active power exchange between the grid and distributed RES and ESS. Advanced grid support capabilities including reactive power regulation require grid-supporting VSCs to also regulate reactive power flow according to reactive power references. Also, weak-grid characteristics and poor grid power quality can make this control function challenging, since the grid voltage magnitude and phase can be polluted by harmonics. Furthermore, when the VSC operates in grid-forming mode, voltage control becomes priority. Generally, it is necessary for voltage, current and power controllers be robust and ensure good power quality with fast dynamic response.

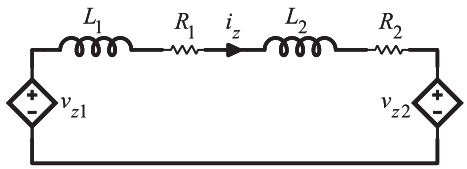

Fig. 3. Equivalent circuit of the zero-sequence dynamics.

2) Power Sharing Among Multiple RES: The power rating or capacity of a single RES/ESS might be insufficient to power the existing and anticipated electrical loads in the microgrid. Therefore, multiple units are installed and are required to share power in proportion to their capacities. Also, the ESS units are required to provide energy that is commensurate to their states of charge [20]. Therefore appropriate control is required to ensure that no RES is overloaded during power sharing. Also, reactive power sharing becomes more challenging when the power lines have unmatched impedances, or when the impedances are unknown [21].

3) Circulating Current Suppression: In modern power electronics-based power systems, parallel-connected ac/dc converters are often employed for higher power capacities. This modular and scalable approach also allows the power conversion systems to achieve flexible installations and low-cost maintenance [22]. Typical applications include grid-connected inverters, active-front-end rectifiers, and electrical drives. Nonetheless, a zero-sequence loop is inadvertently created in parallel ac/dc converters when both ac and dc sides are directly tied together, resulting in circulating current. The suppression of circulating current in parallel ac/dc converters is critical; if not properly regulated, unbalanced power sharing and additional power losses inevitably arise. The equivalent circuit describing the zero-sequence dynamics is shown in Fig. 3, where $v_{z,1}$ and $v_{z,2}$ are the zero-sequence voltage [also called common-mode voltage (CMV)] generated by each ith ac/dc converter ($i \in$

$\{1, 2\}$), and i_z denotes the zero-sequence circulating current. Herein, the definition of zero-sequence components is provided for clarity

$$v_z = \frac{v_a + v_b + v_c}{3}, \quad i_z = \frac{i_a + i_b + i_c}{3}. \tag{1}$$

Specifically, circulating current can be divided into high-frequency circulating current and low-frequency circulating current [23]. The former can be mitigated using advanced PWM techniques [24], [25]. Conversely, low-frequency circulating current requires specific control strategies for its suppression. Linear-based mitigation of circulating current generally incorporate an appropriate zero-sequence current control loop into a classical linear control framework, such as voltage-oriented control. These methods are generally limited by slow dynamic performance.

4) Grid-Fault Ride-Through (FRT): RES and ESS can provide ancillary grid support during faults. This would assist grid-recovery and prevent a potential post-fault grid collapse. Grid faults, which could be symmetrical or asymmetrical, are characterized by moderate to severe voltage sags [26]. Grid codes now require grid-connected converters to remain connected for a specified duration after a fault occurs. This requires in-built capabilities to safely inject reactive power into the grid for specified periods [19], and safely disconnect after the regulatory duration has elapsed without grid recovery. Although microgrids have grid-forming and grid-following converters, the control of grid-fault overcurrents in power-synchronization-based grid-forming converters, in particular, can be challenging [27].

5) Grid Frequency and Voltage Support: Grid-connected RES and ESS are required by IEEE Std. 1547-2018 to provide both frequency and voltage support to the grid through frequency-active power droop and voltage-reactive power droop [19]. Therefore, under conditions of under-frequency, for instance, the converter will regulate injection of extra active power to the grid, to according to the static droop curve. Similarly, in the event of a grid voltage-dip, reactive power injection is required for grid support. Furthermore, the increasing grid-penetration by converter-interfaced energy sources decreases the modern grid's inertia [measured by the rate-of-change-of-frequency (ROCOF)] relative to the traditional synchronous-generator-based power system [28]. Since the grid's stability is better guaranteed when its ROCOF is low, grid-connected converters have the option to provide inertial response by the inertia emulation of the synchronous generator.

6) Power Quality: Power quality challenge is another factor associated with grid-connected microgrids. This is also due to the high penetration of power converters and nonlinear loads that introduce current harmonics that can be inimical to the stability and durability of the loads [29]. Voltage variations/unbalances, and current harmonics are important power quality issues to be mitigated. What is more, source and load uncertainties, weak-grid features, and converter nonlinearities further increase the complexity of solution techniques.

7) Synchronization: Microgrids, owing to the high penetration of converter-interfaced distributed generation, are essentially weak grids. They have low short-circuit ratio due to the high impedance and low inertia, which can result in distorted voltage and frequency. The grid-connected VSCs can be synchronized to the grid by either *voltage-synchronization* or *power-synchronization* for grid-following and grid-forming converters, respectively. Voltage-synchronization is prone to oscillations and instability in weak grids [due to the phase-locked loop (PLL)], while power-synchronization is more stable in weak grids, but suffers from oscillations in stiff-grids [30]. Therefore, selecting the ideal synchronization controller for VSCs in weak grids can be challenging.

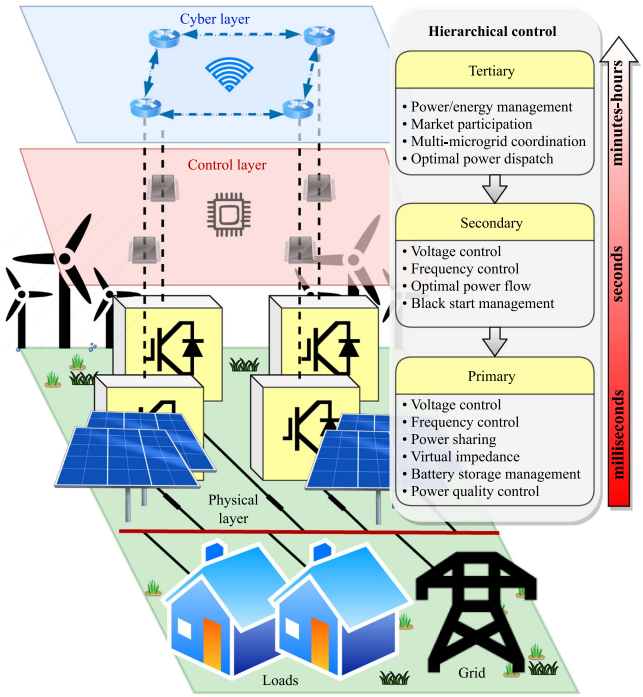

Fig. 4. Hierarchical control of a microgrid.

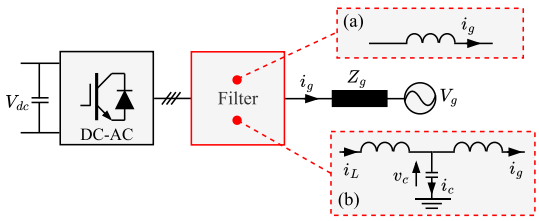

Fig. 5. Grid-connected VSC with filters. (a) *L* filter. (b) *LCL* filter.

C. Control Structures for Grid-Connected Converters

Consider a generic grid-connected power converter in Fig. 5, which has either an *L*-filter or *LCL*-filter. It is common in the literature to have multiple control loops for grid-connected converters, where multiple control objectives are being regulated. The advanced controllers reviewed herein are applicable to the controllers in Fig. 6(a)–(c), where $G_1(s), G_2(s)$, and $G_3(s)$ represent controllers for the first, second, and third control loops, respectively. The example in Fig. 6(d) illustrates how SMC and

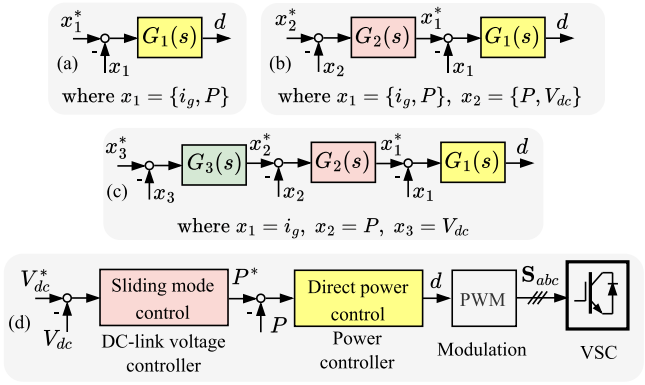

Fig. 6. Control structures for grid-connected power converters, where x^* is the reference for x, and d is the duty cycle. (a) Single-loop controller. (b) Double-loop controller. (c) Triple-loop controller. (d) Example of cascaded double-loop advanced controllers [31].

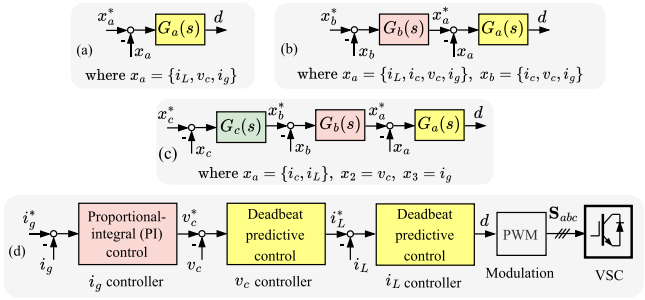

Fig. 7. Control structures for *LCL*-filtered grid-connected power converters, where x^* is the reference for x, and d is the duty cycle. (a) Single-loop controller. (b) Double-loop controller. (c) Triple-loop controller. (d) Example of cascaded triple-loop advanced controllers [32].

DPC both regulate $V_{\rm dc}$ and P, respectively, in cascaded double loops [31].

For the case of *LCL*-filtered VSCs, the advanced control schemes can be used as control stages $G_a(s), G_b(s),$ and $G_c(s)$ in Fig. 7(a)–(c) to regulate the VSC-side inductor current (i_L), grid-side inductor current (i_g) and filter capacitor voltage or current ($v_c$ori_c). Furthermore, an example is shown in Fig. 7(d) where deadbeat predictive control and PI-control are combined in triple cascaded loops to regulate the states of the *LCL*-filtered VSC.

III. Grid-Synchronization Stability

Fig. 8(a) shows a grid-connected VSC that injects current $I_o\angle\theta_o$ into the point of common coupling (PCC). The dynamic stability of the system will be investigated for the case when a grid-fault causes a low voltage V_F to occur as shown. Both the steady-state model and *quasi-static* model lead to identical steady-state power transfer limit criteria, however, the latter is further discussed because it can reveal dynamic stability criteria through the PLL dynamics.

When the inner current loop's bandwidth is much higher than the PLL's, the current loop can be replaced with a current-controlled current source. Expressing the PCC voltage in the synchronous reference frame of the PLL, the $q-$axis component

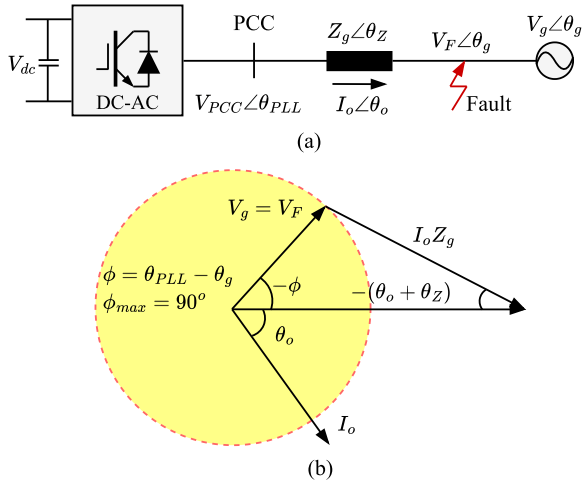

Fig. 8. Grid-connected power converter synchronization dynamics. (a) Network line diagram. (b) Phasor diagram of current injection $I_o\angle\theta_o$ where V_F is a constant magnitude fault voltage.

is

$$V_{\text{PCC},q} = V_g \sin(\theta_g - \theta_{\text{PLL}}) + Z_g I_o \sin(\theta_o + \theta_Z) \quad (2)$$

where θ_g is the angle of the grid voltage and $\theta_{inj} = \tan^{-1}(i_q^{\text{ref}}/i_d^{\text{ref}})$ is the angle of the injected current reference relative to the PLL phase angle. At the incidence of a fault with resistive impedance $R_f \approx 0$, the grid voltage is replaced by nearly zero, constant magnitude fault voltage V_F. The relationships of these vectors are depicted by the phasor diagram Fig. 8(b).

The first term of (2) can be regulated by the PLL to ensure that $V_{\text{PCC},q} = 0$. The second term is a positive feedback disturbance that the PLL needs to cancel in order ensure stability. Therefore, the limit of injected current is given by

$$I_{o(\text{limit})} < \frac{V_g}{Z_g \sin(\theta_o + \theta_Z)}. \quad (3)$$

Also, the steady-state limit of current magnitude during the fault is

$$I_{o(\text{fault limit})} = \frac{V_F}{R_F}. \quad (4)$$

In summary, (3) and (4) indicate that loss of synchronization is determined by: 1) high grid impedance Z_g, 2) low grid voltage $V_g = V_F$, 3) the magnitude of injected current, and 4) mainly the line resistance during low-voltage faults. The first two reasons are associated with low short-circuit ratio grids.

Several solutions in the literature have been proposed to mitigate grid-synchronization instability of grid-connected grid-forming and grid-following power converters. In particular, small-signal stability analysis and large-signal (or transient) stability analysis are respectively applied to small grid-disturbances and large/severe grid-disturbances, as summarized in Table I.

TABLE I
SMALL-SIGNAL AND LARGE-SIGNAL GRID-SYNCHRONIZATION INSTABILITY MITIGATION FOR GRID-CONNECTED POWER CONVERTERS

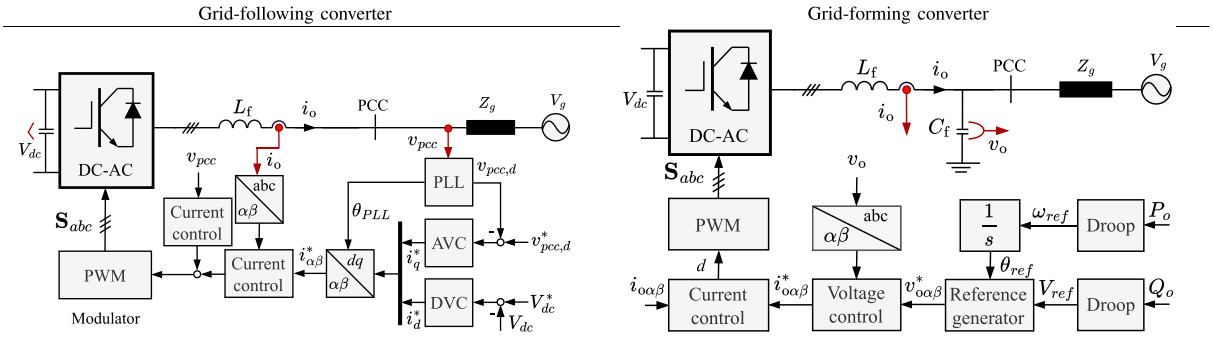

Grid-following converter		Grid-forming converter	
Problem(s)	Small-signal stability solutions	Problem(s)	Small-signal stability solutions
Sideband oscillation:	✓Virtual impedance shaping [33] ✓Feedforward from the PLL [34] ✓Reduction of PLL bandwidth [35] ✓Modified PLL structure [36]	*Sideband oscillation:*	✓Reduction of power loop gains [37] ✓Power control lead-lag compensation [38]
		Synchronous oscillation:	✓Power loop phase compensation [39] ✓Virtual impedance shaping [40]
Large-signal stability solutions		Large-signal stability solutions	
✓Freeze the PLL [41] ✓Equal area criterion frequency control [42] ✓Switch PLL to first-order model [43] ✓Increase active current/power with PLL frequency error [44]		✓Actively damp the transient response [45] ✓Switch to first-order power control [46] ✓Reduce active power reference [47] ✓Increase reactive power reference [48]	

*AVC is alternating voltage control, DVC is direct voltage control, and PLL is phase-locked loop.

A. Small-Signal Stability

Small-signal stability of grid-following converters involves different schemes aimed at reducing the sideband oscillations which arise from asymmetrical control loops of the grid following converter in grids characterized by low short-circuit ratios. Impedance-based analysis sheds light on the PLL's negative damping as a negative low-frequency resistance that is inimical to the converter's stability [30]. Impedance-shaping to reducing the PLL's negative resistance through virtual-impedance-based voltage feed-forward from the PCC voltage was proposed in [33]. Applying feedforward from the PLL can be used to achieve symmetrical dq dynamics, improving small-signal stability [34]. Reducing the PLL's bandwidth also helps to mitigate the side-band oscillations by limiting the active bandwidth of the negative resistance.

Grid-forming converters have small-signal synchronization instability induced by both side-band oscillations and synchronous oscillations [30]. Side-band oscillations can be mitigated by reducing the power controller loop gains [37] and introducing active/reactive power control lead-lag compensation [38]. The latter method is limited because it enhances coupling between active and reactive power control loops. Synchronous oscillations can be mitigated by simply adding a virtual impedance as a form of active damping [40]. Also a damping approach based on virtual mechanical inertia or adding virtual electrical resistance is proposed in [49], while Li and Li [39] proposed reducing the active and reactive power cross-coupling through proportional damping terms. Nonetheless, this method does not nullify the cross-coupling.

B. Large-Signal Stability

Severe grid faults and nontrivial load/generation changes are large disturbances that alter the equilibrium points of the power system, necessitating transient stability analysis. Transient stability of the grid-following converter is ensured by: 1) modifying the injected active current vector or active power and 2) by modifying the parameters of the PLL. A fundamental approach using the first group of solutions is to reduce injected active current in proportion to the grid-voltage drop [30]. Nonetheless, since there is still some amount of active current, it hinders the injection of absolutely reactive current. More recent approaches increase active current/power references in proportion to the PLL frequency error [44], [50], resulting in stable operating area. The equal area criterion was proposed in [42] for dynamic active power balance. The decelerating or accelerating area at the instance of the transient period is regulated by proportional–integral control of the frequency deviation to prevent the operating point from getting into the negative damping zone. The second category of solutions which adjust the PLL include freezing the PLL during the fault [41] and switching the PLL from the second-order dynamics to first-order model [43]. Generally, the PLL-adjusting methods are effective in stabilizing perturbed systems to an equilibrium point, from which further control action can be taken.

Transient stability of grid-forming converters is achieved by dynamically changing active/reactive power references, and by modifying the order of the controller. Similar to the operation of synchronous generators, reducing active power reference (to decelerate the machine) and increasing reactive power references (to increase voltage) during grid faults, all work to sustain synchronization stability [47], [48]. Although second-order or higher order power controllers produce better frequency response, first-order power controllers give better transient stability to grid-forming converters. Therefore, reported interventions include active damping [45] of the transient response of the second-/higher order controller and switching to first-order power control during transients [46].

IV. Motivation for Advanced Control of Microgrids

This section presents the motivation for advanced hierarchical control of sustainable microgrids. The control objectives of the different hierarchical levels are discussed, as well as the limitations of linear control in microgrids.

A. Hierarchical Control of Microgrids

The electrical variables in microgrids, e.g., frequency, voltage, active/reactive power, are regulated at different bandwidths and timescales. So, it is convenient to categorize these variables into different groups (see Fig. 4) according to their relative timescales of regulation, namely: *primary, secondary, and tertiary* control hierarchies [51], [52].

The primary hierarchy of control usually regulates the microgrid's states at the typical time-scales for switching power electronic converters, i.e., *milliseconds to seconds*. The converter frequency and output voltage magnitude provide references for current and voltage control loops. Active/reactive power sharing among multiple converters in the network is also done by methods like droop control. Other high-level control objectives include virtual impedance, power quality, battery charging/discharging, and islanding detection.

The secondary control hierarchy guarantees the integrity of the microgrid by restoring voltage and frequency to the appropriate reference values. The control is decoupled from the primary hierarchy by operating at a lower bandwidth and timescale around *several seconds to minutes*. Additional control objective include regulation of real/reactive power, grid-synchronization, and black start management [52].

Tertiary control oversees higher level objectives than the lower hierarchies, at a slower time scale of *minutes to hours*. The control objectives include market participation, optimal power dispatch, and multimicrogrid coordination.

B. Limitations of Linear Control Methods

The multiloop controlled *LC*-filtered VSC in Fig. 9(a) is a common configuration of voltage-controlled grid-forming VSCs. The outer loop is a basic droop $P-f, Q-V$ controller, and the linear-based inner loop consists of voltage and current controllers $G_v(s)$, $G_i(s)$ in cascade, respectively. $G_i(s)$ operates at a faster bandwidth than $G_v(s)$. The output of $G_i(s)$ drives the pulsewidth modulator to regulate the average output voltage during each sample period.

Fig. 9(b) shows the bandwidth scales of the cascaded linear control blocks. Assuming that the current loop operates at a decade lower than the sampling frequency f_s (converter switching frequency is f_{sw}), to facilitate decoupling of the control loops, the voltage loop will operate at a bandwidth of $f_s/100$. Thus, the overall system's bandwidth will be about two to three orders of frequency lower than f_s, resulting in a slower dynamic response. Herein lies a key limitation of linear control of multihierarchical, multitime-scale microgrids.

Microgrids operate in multiple hierarchies, with the VSC control being the primary control layer. Therefore, if the primary control can be designed with faster bandwidth, the secondary and tertiary hierarchies will be capable of operating with improved dynamic response. Several studies agree that multiple-input multiple-output control, e.g., MPC, does not require cascaded voltage/current control loops for VSCs, and has higher bandwidth and faster dynamic response than linear control schemes [53], [54], [55]. For instance, the bottom two bandwidth scale plots of Fig. 9 show that nonlinear control, which obviates a dedicated PWM stage, can increase the VSC's primary control bandwidth by an order of up to two decades. Thus, outer control loops (of the primary hierarchy), as well as the secondary and tertiary hierarchies can operate at faster control bandwidths than linear control.

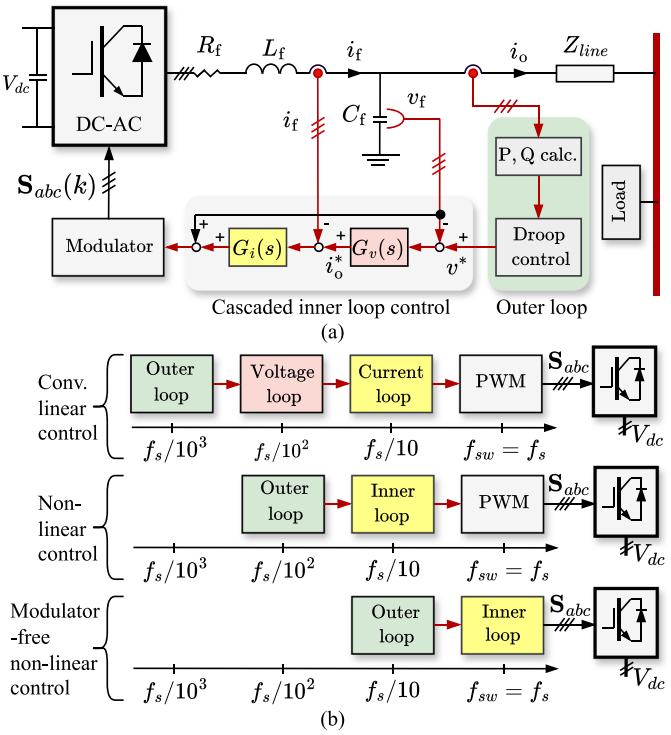

Fig. 9. Linear control of a VSC and the bandwidth. (a) Schematic diagram of linear control. (b) Bandwidths of control loops.

Additional desirable features of modern controllers include explicit inclusion of constraints (physical limits on the inputs or their rate of change and outputs) in the design process, the possibility of utilizing information on future references, and compensating for disturbances. Linear controllers, e.g., PID controllers, do not permit these features conveniently. For instance, the inability to specify explicit constraints in the design process limits the safe application of linear control. A recent solution has been proposed to circumvent violations to input or output constraints in [56]. It utilizes a quadratic programming solver to compute the optimal control input with respect to the plant's constraint function, and the permissible bounds on the control input. The challenge with this approach is that the online optimization is carried out after the classical closed-loop control design has been completed. Thus, the modified optimal control input might no longer satisfy initial stability margins or dynamic response requirements.

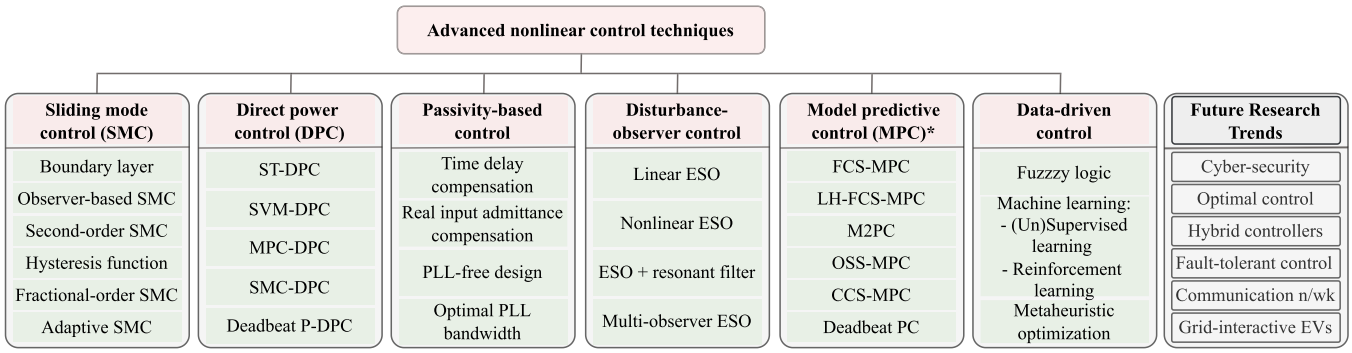

Fig. 10. Reviewed advanced control methods and future trends. ST-DPC is switching table DPC, SVM-DPC is space vector modulator DPC, SMC is sliding mode control DPC, FCS-MPC is finite control-set MPC, LH is long-horizon, M2PC is modulated MPC, OSS-MPC is optimal switching-sequence MPC, and CCS-MPC is continuous control-set MPC. *MPC refers to *nonlinear* MPC.

The control methods discussed in the following sections are with respect to primary control objectives.

V. Introduction to Advanced Control Methods

The leading advanced control methods for grid-connected power converters, shown in Fig. 10 are introduced, with particular attention to their fundamental operational principles.

A. Sliding Mode Control

SMC has emerged as a popular control method due to its simplicity, order reduction, decoupling of state variables, and robustness to uncertainties and exogenous disturbances. Nonetheless, its well-known chattering limitations, which decrease performance and increase thermal losses, have made chattering reduction/elimination one of the most researched aspects of SMC. The fundamental principle of SMC for a nonlinear system is that the control input $u_i(t)\ \forall\ i \in [1, 2, \ldots, n]$ should make the state variables reach the sliding surface, and be maintained along the same surface

$$u_i(t) = \begin{cases} u_i^+(t), & \text{if } S_i(x) > 0 \\ u_i^-(t), & \text{if } S_i(x) < 0 \end{cases} \tag{5}$$

where $\{u_i^-(t), u_i^+(t)\} : u_i^-(t) \neq u_i^+(t)$ are distinct control inputs and $S_i(x) \in \mathbf{S}(x) = [S_1, S_2, \ldots, S_n]^\top$ is the switching vector; $\mathbf{S} = \mathbf{0}$ is the sliding surface. The necessary and sufficient condition for *reachability* is

$$\mathbf{S}(x)\dot{\mathbf{S}}(x) < 0. \tag{6}$$

B. Direct Power Control

DPC stems from the instantaneous power theory [57], [58], and directly controls the active power (P) and reactive power (Q) of pulsewidth modulated converters. Its fundamental implementation is characterized by fast dynamic response, simple structure, no separate PWM block or coordinate transformation. These features make DPC preferred to VOC which has lower input power factor and more complex algorithms for coordinate transformation and decoupling of P and Q.

The complex power $\mathbf{S}$ of a three-phase system is the dot product of the voltage and conjugate current vectors, i.e.,

$$\mathbf{S} = \frac{3}{2}(\mathbf{e}.\mathbf{i}^*) \tag{7}$$

where $\mathbf{e}$ is the supply voltage vector, $\mathbf{i}$ is the converter current, and $\{\}^*$ is the conjugate operator. The rate of change of $\mathbf{S}$, $d\mathbf{S}/dt$ gives the respective instantaneous active and reactive powers as

$$\begin{cases} \frac{dp}{dt} = \frac{3}{2L}E^2 - \frac{V_{dc}E}{L}\cos(\omega t + \theta_E - \frac{\pi}{3}(k-1)) - \frac{Rp}{L} - \omega q \\ \frac{dq}{dt} = -\frac{V_{dc}E}{L}\sin(\omega t + \theta_E - \frac{\pi}{3}(k-1)) - \frac{Rq}{L} - \omega p \end{cases} \tag{8}$$

where $\mathbf{e} = E\cos(\omega t + \theta_E)$, $\{R, L\}$ are the filter resistance and inductance, respectively, and V_{dc} is the dc-link voltage. The classical DPC (ST-DPC) introduced in [58] employs a hysteresis controller and uses a switching table (ST) to determine switching states. More recently, DPC has been significantly enhanced while preserving the advantages of the underlying concept.

C. Disturbance-Observer-Based Control

DOBC techniques operate on the principle of estimating the disturbances in the system, and compensating for them to either eliminate or attenuate their impact. The disturbances are broadly classified as both external disturbance and internal disturbance–including parameter uncertainties, unmodeled dynamics and measurement noise. Observers (linear and nonlinear) are necessary to estimate the so-called *lumped disturbance* [59] since the latter could either be too expensive or practically impossible to measure directly.

Given a nonlinear system to be controlled by the DO method. Its output y is tainted by the measurement noise $\mathcal{N}$. The disturbance observer, whose operation is triggered when the physical system is mismatched with the nominal model, provides an estimate of the lumped disturbance $\hat{d}$. The inner feedforward loop then rejects the disturbance d, while attenuating uncertainties too. A key advantage of DOBC over other techniques is that it provides two-degrees of freedom—for feedback control and disturbance rejection—obviating tradeoff between the nominal control performance and robustness. Therefore, DOBC has grown in popularity for its simplicity, robustness and superior dynamic performance. The increasing importance of

DO-based methods is further solidified by their ease to complement other nonlinear control methods, such as SMC and MPC. Furthermore, DOBC's development has matured for industry adoption [3].

The rest of this section will be discussed for the case of a single-input-single-output nonlinear system defined by

$$y^{(n)}(t) = g\left(y(t), \dot{y}(t), \ldots, y^{(n-1)}(t), d(t), t\right) + \alpha u(t) \quad (9)$$

where $y^{(j)}$ is the jth derivative of y, u is the control input, d is the disturbance, and α is the input gain.

The estimation of disturbance can be achieved with the DO in either the frequency domain or time domain. The frequency DO is convenient to apply in that it requires only the system's input/output, but it is limited because it is mainly applicable to minimum-phase systems with matched disturbances. The time-domain DO is suitable for both (non-) minimum-phase systems, as well as mismatched disturbances; but it requires detailed information of the system's states [59].

The extended state observer (ESO) provides a compact scheme for estimating both the states and lumped disturbance with limited information about the system's model. The ESO, whose equivalence to the generalized proportional–integral observer has been shown [60], is fundamental to active disturbance rejection control–which linearizes a nonlinear system into perturbed chains of integrators [3].

1) Linear Extended State Observer (LESO): If the lumped disturbance is considered to include the nonlinear unmodeled dynamics of the system, the linear ESO can be applied to estimate the states and lumped disturbance. Define the states $z_1 = y,\ z_2 = \dot{y},\ \ldots, z_n = y^{(n-1)}$ and extended state z_{n+1}; leading to the (extended) state equations [61]

$$\begin{cases} \dot{z}_i = z_{i+1}\ \forall\ i \in [1, 2, \ldots, n-1] \\ \dot{z}_n = g(z_1, z_2, \ldots z_n, d, t) + \alpha u \\ \dot{z}_{n+1} = m(t):\ m(t) = \dot{g}(z_1, z_2, \ldots z_n, d, t). \end{cases} \quad (10)$$

The corresponding classical linear ESO to give the estimate $\hat{z}_j$ of the extended states (disturbances) z_j in (10) is

$$\begin{cases} \dot{\hat{z}}_i = \dot{\hat{z}}_{i+1} + \varrho_i(y - \hat{z}_1) \\ \dot{\hat{z}}_{n+1} = \varrho_{i+1}(y - \hat{z}_1) \end{cases} \quad (11)$$

where $\{\varrho_i\ , \varrho_{i+1}\}$ are the ESO gains designed to ensure asymptotic convergence of $\hat{z}_i \to z_i$, and $\hat{z}_{n+1} \to z_{n+1}$. The classical linear ESO has shortfalls including trading off disturbance rejection for measurement noise suppression; several recent improved ESOs are reviewed in Section VII-C.

2) Nonlinear ESO: Since the system in consideration is nonlinear, a linear observer ignores the nonlinear dynamics, resulting in limited estimation accuracy. The estimation accuracy of the lumped disturbance can be improved by including the known nonlinear dynamics in the estimation process; this necessitates the nonlinear ESO. Nonlinear ESOs have the general structure

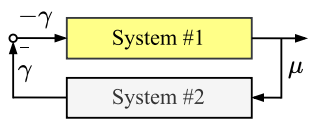

Fig. 11. Negative feedback interconnection of two systems.

$$\begin{cases} e_{rr} = y - \hat{z}_1 \\ \dot{\hat{z}}_i = \dot{\hat{z}}_{i+1} + \mathcal{M}_i(e_{rr})e_{rr} \\ \dot{\hat{z}}_{n+1} = \mathcal{M}_{i+1}(e_{rr})e_{rr} \end{cases} \quad (12)$$

where $[\mathcal{M}_i(e_{rr}),\ \mathcal{M}_{i+1}(e_{rr})]$ are nonlinear gain functions designed to ensure asymptotic convergence of $\hat{z}_i \to z_i$, and $\hat{z}_{n+1} \to z_{n+1}$.

D. Passivity-Based Control

PBC of microgrids, and grid-tied power converters is introduced in the following.

1) Passivity Principles for Microgrids: Passivity relates nicely to Lyapunov stability and provides a useful tool for analyzing nonlinear systems. Passivity requires that the phase of transfer functions be less than 90° so that the loop phase is strictly less than 180°. The main theorem of passivity states that the (negative) feedback connection of two passive systems is passive [62]. Thus, passivity approaches can be applied to inverter-based microgrids by separating the system into two distinct subsystems connected via a negative feedback as in Fig. 11. In particular, *System 1 := Inverter dynamics; System 2 := Network dynamics* [12], where the network dynamics incorporate load and line dynamics. The network input and output are $w = \mu$ and $y = \gamma$, respectively, while for inverters the input and output are $w = -\gamma$ and $y = \mu$, respectively. The inverter and network dynamics are said to satisfy passivity properties if their respective dynamical systems satisfy passivity as defined in Definition 1 below.

To formalize the notion of passivity, consider the negative feedback interconnection of two subsystems (see Fig. 11). Let each subsystem be described by a dynamical system represented by the state space model

$$\dot{x} = f(x, w), y = h(x, w) \quad (13)$$

where $x(t) \in \mathbb{R}^n$ is the state vector, $w(t) \in \mathbb{R}^m$ is the input vector, and $y(t) \in \mathbb{R}^p$ the output vector. $f : \mathbb{R}^n \times \mathbb{R}^m \to \mathbb{R}^n$ and $h : \mathbb{R}^n \times \mathbb{R}^m \to \mathbb{R}^m$ are locally Lipschitz and continuous, respectively. Passivity is defined as follows.

Definition 1 (Passivity): Consider a dynamical system as in (13). Let (x^*, w^*) denote the equilibrium point of x, w. Let the deviations of x, w from the equilibrium point (x^*, w^*) be $\tilde{x} = x - x^*$, $\tilde{w} = w - w^*$, respectively. The system (13) is said to be locally passive about the equilibrium point (x^*, w^*) if there exists a continuously differentiable positive semidefinite function $\mathcal{H}(\tilde{x})$ such that, for all x, w, $\dot{\mathcal{H}} \leq \tilde{w}^\top \tilde{y}$; it is locally strictly passive if $\dot{\mathcal{H}} \leq \tilde{w}^\top \tilde{y} - \tilde{x}^\top \phi(\tilde{x})$ where ϕ is a positive definite function; and it is locally output passive if $\dot{\mathcal{H}} \leq \tilde{w}^\top \tilde{y} - \tilde{y}^\top \rho(\tilde{y})$

where ρ is a positive definite function. Other cases of passivity can be found in [62, Def. 6.3].

By representing the network dynamics, as in (13), in the common reference frame [12], [13], it holds that the network is strictly passive as in Definition 1 (see e.g., [12], [13]). Therefore, by exploiting the passivity properties of the network, it is sufficient to guarantee the stability of microgrids by demanding that the inverters are *passive*, *strictly passive* or *output strictly passive*, as in Definition 1. As a result, passivity-based techniques allows to design inverter controllers that are line-independent, thereby leading to high-performance and scalable microgrids with plug-and-play capabilities. Passivity-based controllers for inverters can differ in architecture, namely, those with single loop [11], [13] and double loop [12]. These have been designed to be *passive* as in [11], *strictly passive* as in [12], and *output strictly passive* as in [13]. A detailed description of those can be found in the respective literatures.

2) PBC of Grid-Tied Power Converters: Passivity theory has been demonstrated as an effective approach to analyze the stability of grid-connected microgrids, which have a high penetration of grid-tied VSCs [63]. Given a microgrid with large number of VSCs, as long as each VSC remains passive—by keeping the real part of the input admittance nonnegative at all frequencies up to the Nyquist frequency, or at least at the critical frequencies at which resonance instability can be induced—stability can be guaranteed. Resonance-induced instability can arise from time delay, inner current controller dynamics and the outer controller dynamics comprising the phase-locked loop (PLL), and voltage controller. These factors can cause both harmonic and near-synchronous resonances [63].

Therefore, the specific key passivity control objectives are: 1) to reduce the total time delay, 2) proper compensation of the real-part of the input admittance, 3) selection of an appropriate bandwidth for the outer loop, and 4) avoiding PLL's influence (by methods e.g., DPC, designing in the stationary reference frame, etc). These lead to four corresponding groups of solutions for passivity in VSCs, discussed in Section VII-D.

E. Model Predictive Control

MPC is a multiobjective receding horizon scheme that seeks an optimal control input sequence $\mathbf{U}_{\text{opt}}(k)$ from the input space $\mathbf{U}(k) = [\mathbf{u}^T(k)\ \ \mathbf{u}^T(k+1)\ \ \dots\ \ \mathbf{u}^T(k+N_p-1)]$ to minimize the cost function J of the optimization problem over a prediction horizon $N_p \in \mathbb{N}$ time steps. $\mathcal{X}$ and $\mathcal{U}$ are the state and input constraints sets, respectively

$$\mathbf{U}_{\text{opt}}(k) = \min_{\mathbf{U}(k)} J \quad \text{s.t. } x(k) \in \mathcal{X}, u(k) \in \mathcal{U} \tag{14}$$

$$J = \sum_{k=1}^{k+N_p-1} \|\mathbf{y}^p(k+1) - \mathbf{y}^*(k+1)\|_2^2 + \lambda_{\text{u}} \|\Delta u(k)\|_2^2 \tag{15}$$

where $\mathbf{y}^p$ is the predicted output which is derived from the system's mathematical model, $\mathbf{y}^*$ is the reference, $\lambda_{\text{u}} \in \mathbb{R}^+$ penalizes the control effort $\Delta u(k) := u(k) - u(k-1)$, $\|\boldsymbol{\zeta}\|_2^2$ is the squared l_2-norm of vector $\boldsymbol{\zeta} = [\zeta_1, \zeta_2, \dots, \zeta_n]^\top$ defined as $\|\boldsymbol{\zeta}\|_2^2 = \zeta_1^2 + \zeta_2^2 + \dots + \zeta_n^2 = \boldsymbol{\zeta}^\top \boldsymbol{\zeta}$. Only the first term of the sequence $\mathbf{U}_{\text{opt}}(k)$ is applied to the plant and the measurement/estimates of the states are used to compute the next sampling instant's predictions and optimal sequence.

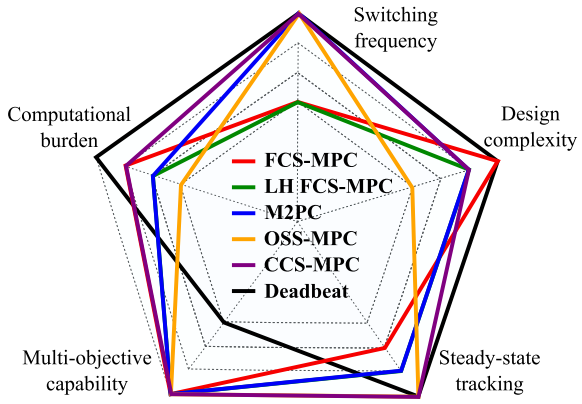

Fig. 12. Features of MPC methods. Performance range: poorest (innermost polygon) to best (outermost polygon). LH is long-horizon, M2PC is modulated MPC, OSS-MPC is optimal switching-sequence MPC, and CCS-MPC is continuous control-set MPC.

In power electronic applications, although the system's model is usually linear [64], nonlinear MPC (having nonlinear cost function) is most commonly used. It has been established that when more than one objective is to be controlled, nonlinear cost functions, which can also include nonlinear constraints, produce more stable and optimal results [64], [65]. MPC's key advantage over other advanced control methods lies in its capability for multiobjective control with constrained optimization. The same cost-function for a converter topology can be used to achieve primary control objectives, such as current, voltage, and power control, as well as secondary objectives including dc-link capacitor voltage control, thermal stress balancing, and switching frequency reduction. For instance, the cost function can be used for voltage control and thermal stress balancing in hybrid active neutral-point-clamped (NPC) converters to prolong the lifetime of the most-thermally stressed devices [66]. MPC is also beneficial when combined with other advanced control methods, e.g., MPC reduces the power ripples and current THD of DPC by duty-optimized multivectors per sampling interval (see Section V-B). What is more, MPC's development has matured for industry adoption, in particular, the model predictive pulse pattern control [4] and its recent adaptation for grid-connected converters [67].

MPC techniques fall into two main groups: CCS-MPC, also called indirect MPC and finite control-set MPC (FCS-MPC), also called direct MPC. CCS-MPC separates the computation of the control action and modulation into sequential steps, and thus requires a dedicated modulator. However, FCS-MPC combines both control and pulsewidth modulation into the same scheme. Due to its ease of designing multiobjective problems, computational realizability for high-dimensional systems, and suitability for time-varying references, FCS-MPC is the more popular of the two groups [7]. Fig. 12 shows the different variants of MPC

and their relative performance features. Further MPC schemes for grid-tied converters and microgrids are provided in [68], [69], and [70].

F. Data-Driven Control Techniques

Popular data-driven methods include fuzzy logic, metaheuristic optimization and machine learning [comprising supervised/unsupervised learning and reinforcement learning (RL)]. Fuzzy logic is based on rules that introduces *fuzziness* into Boolean logic through a process known as *fuzzification*. This fuzziness is employed to gauge the certainty and precision within decision-making domains, resulting in what are termed *fuzzy variables*. Following fuzzification, these fuzzy variables undergo defuzzification to produce crisp values. The advantage of this technique is its greater simplicity and ease of interpretability over many other data-driven methods.

Machine learning is typically categorized into three main types: supervised learning, unsupervised learning, and RL. The goal of supervised learning is to establish the relationship between input and output data. It typically involves two primary tasks depending on the type of output data: classification and regression. Classification deals with output in finite and discrete forms, making it suitable for categorizing data into classes. Conversely, regression deals with output in continuous values. ANN is the most popular machine learning approach for establishing relationships between input and output data. ANN comprises three fundamental layers: the input layer, hidden layers, and output layer. DNN has two or more hidden layers, while convolutional neural network (CNN) is specialized in processing grid-like data and excel in spatial pattern recognition. In an ANFIS, fuzzy logic inference occurs within a neural network framework. In ANFIS, neural networks learn and optimize the parameters of the fuzzy logic system.

Unsupervised learning does not rely on labeled datasets. Instead, it is commonly used for labeling data autonomously. Many machine learning clustering methods fall under unsupervised learning, such as k-means clustering, which groups data by minimizing deviations among them. Metaheuristic methods, employ heuristic approaches to efficiently find solutions that are close to optimal. For instance, the particle swarm optimization (PSO) mirrors the social behavior observed in flocks of birds and schools of fish. PSO involves simulating multiple individuals termed "particles," monitoring their interactions and movements within the design space. This iterative process persists until predefined convergence criteria are satisfied.

Table II shows the summary of the reviewed methods, with details on their advantages and disadvantages. Detailed discussions follow in Sections VI and VII.

VI. Recent Advances in the Control of Grid-Connected VSCs

The application of advanced control techniques to the control objectives of grid-connected VSCs earlier introduced in Section II are covered in this section.

A. Voltage, Current, and Power Control

Current, voltage, and power need to be regulated at their reference values with high precision, low THD, fast dynamic response and excellent steady-state and dynamic performances. Liu et al. [84] proposed the PBC-based current control of a single-phase *LCL* filtered VSC for traction power grid. Active and reactive power decoupling was done by a Euler–Lagrange model in the synchronous frame. Passivity-based active damping suppressed current harmonics, while ensuring fast dynamic response at a high stability margin. The generalized application of PBC to both grid-forming and grid-following VSCs was proposed in [85]. Another generalized PBC approach from the perspective of admittance model was proposed in [88]. In particular, the novel model eases the flexible choice between VSC-current control and grid-current control. The use of a Luenberger observer further improves disturbance rejection. Quasi-integral sliding mode power control with super-twisting observer improves the overall steady-state power and voltage performances, while sustaining the robustness and fast dynamic performance of SMC [103].

The steady-state current tracking performance of MPC was improved in [104] by the use of an ESO to estimate the overall disturbances and compensate for the tracking error associated with conventional MPC. MPC-based DPC was proposed in [105] with advantages of reduced ripples at lower switching frequencies (MPC_2 in Fig. 20) than DPC or coventional MPC (MPC_1). However, it is limited by the weaknesses of the conventional ESO. Therefore, a novel parallel-cascade ESO improved predictive current control with robustness to measurement noise, unmodeled dynamics and parameter mismatches was proposed in [106]. The combined use of PSO and fuzzy for the optimal auto-tuning of proportional–integral controller gains for active and reactive power control was reported in [107] with robust, low-ripple steady-state results and faster transient convergence than the classical methods.

B. Grid-FRT

Regulatory FRT requirements impose both internal and external control demands on the VSC: protection from fault overcurrents, and reactive power support. A holistic approach in to FRT for grid-tied systems entails fast grid-fault detection, seamless transition between PV's maximum power-tracking mode and FRT mode, and adaptive reference computation for active and reactive power (based on the mode of operation) [108]. A hybrid FRT scheme that employs fuzzy logic and posicast control was applied in [109] to mitigate shallow and deep voltage sags in the series VSC for a grid-connected DFIG wind turbine. ANFIS was combined with DPC in [110] for DFIG's grid FRT with reduced active/reactive power overshoot and settling time during grid fault transients. Other data-driven studies for fault diagnosis in the FRT scheme of grid-connected converters include CNN [111] and fuzzy logic [112].

A classical SMC was applied to FRT for PV VSC; although robust, high dynamic performance was reported, it is limited by SMC's chattering limitations. Further work on DFIG's FRT in [113] employed the event-triggered SMC with DOBC.

TABLE II
SUMMARY OF REVIEWED ADVANCED CONTROL METHODS

Method	Approach	Advantages	Disadvantages
SMC	Observer-based [71], [72]	Good disturbance rejection; fixed switching frequency.	Medium complexity.
	Second-order SMC [73]	Finite convergence time; good robustness.	Chatters under large disturbances.
	Hysteresis function [74]	Low complexity.	Variable sw. frequency; steady-state error.
	Fractional-order [75]	Good disturbance rejection.	High complexity.
	Adaptive SMC [76]	Low to medium computational burden.	Medium to high complexity.
DPC	Space-vector modul. [77]	Constant switching frequency.	Multiple reference-frame transformations.
	Deadbeat predictive [78]	Constant switching frequency; low power ripples.	Sensitive to parameter uncertainties.
	Gradient correction [79]	Improved robustness; online parameter identification.	Higher computational burden.
	Grid-voltage modulation [77]	Less reference-frame transformations; avoids PLL.	Medium complexity.
	Observer-based [73], [80]	Improved robustness to measurement noise.	Higher computational burden.
DOBC	Gen. integral ESO [81]	Can estimate fast-varying disturbances.	Relies on PLL; medium complexity.
	Resonant ESO [82]	Adaptive to grid frequency changes.	Effective for predictable disturbances.
	Multifrequency ESO [83]	Robust to measurement noise.	Medium to high complexity.
	Sliding mode observer [73]	Robust to parameter uncertainties.	Not robust to unmodeled dynamics.
PBC	Power decoupling [84]	Robust to uncertainties/external disturbances.	Relatively higher complexity.
	Port-Hamiltonian [85]	Robust stability; simplified stability analysis.	Conservative; trades off dynamic response.
	Damping injection [86], [87]	Prevents *LCL*-filter resonance instability.	Admittance models are restricted.
	General admittance model [88]	Flexible for passivization with multiple variables.	–
MPC	Weighting-factor free [89]	Simplicity and computational efficiency.	Not robust to uncertainties.
	Prediction error correction [90]	Improved robustness.	Not robust to unmodeled dynamics.
	Ultralocal model/observer [91]	Robust to multiple uncertainties.	Medium to high complexity.
	Passivity-damped MPC [92]	Improved robustness/steady-state performance.	Increased complexity.
	Data-driven emulator [93]	Robust and computationally-efficient.	Requires extensive data for training.
	Sphere-decoding [94]	Computationally-efficient for high-power.	Limited robust performance.
Data-driven	Fuzzy logic [76], [95], [96]	1. Handles uncertainty and imprecision well. 2. Easy to understand. 3. Simple implementation.	1. Rule creation needs expert knowledge. 2. Complex when many rules are required.
	Neuro-fuzzy [97]	1. Can adapt to new data through learning.	1. Computationally intensive training.
	ANN [98], [99]	1. Good at handling non-linear relationships. 2. Highly flexible and adaptable.	1. Requires large data-sets for training. 2. Computationally intensive.
	Physics-informed-NN [100]	1. Incorporates physical laws into learning. 2. Can generalize better with less data.	1. Requires knowledge of the underlying physical laws. 2. May be complex.
	Bayesian network [101]	1. Has probabilistic reasoning; handles uncertainty. 2. Good for small datasets.	1. Computationally expensive for large networks. 2. Requires expert knowledge.
	Particle swarm optm. [102]	1. Simple and easy to implement. 2. Finds global optima effectively.	1. Can converge prematurely. 2. Performance depends on parameter settings.
	Reinforcement learning [20]	1. Learns optimal policies through interaction with the environment. 2. OK for complex environments.	1. Requires large amounts of data. 2. Computationally intensive.

DC-link voltage regulation had minimal chattering and greater control efficiency than classical SMC, since the control input is only refreshed under violation of the stability conditions. A comparative study on overcurrent limiting capability for power synchronization virtual synchronous generator (VSG) in a grid-connected grid-forming converter was reported in [114]. It was shown that while virtual impedance current limiting and a multiloop methods have effective current-limiting capabilities, FCS-MPC outperformed them in transient response of active and reactive power after fault clearance.

C. Power Quality Issues

High power quality is a fundamental control requirement in a microrid with high-penetration of converter-interfaced RES. Weak grids commonly have asymmetrical voltage dips [79], and switching converter-induced current harmonics, which can degrade the VSC's filter and load. Therefore, active control is required to compensate for the unbalances and suppress harmonics too. Zhang et al. [79] proposed DPC with gradient-correction online inductance-identification. The real-time inductance computation improves robustness over the classical DPC technique. Unbalance and harmonics are compensated with terms derived from the extended power theory to determine revised reference voltage vector. Finally, power ripples are minimized by the space vector modulation of the calculated voltage vector, improving the overall. The harmonic compensation scheme in [79] was extended in [78] to achieve model-free predictive current control with unbalance and distorted grid voltage compensation. Similarly, Mohapatra and Agarwal [115] proposed the reduction of active power ripples under distorted grid conditions, within an MPC framework. Positive and negative sequence components of the distorted grid voltage were first computed in [116]

for compensation in SMC framework. Super-twisting current control combined with outer-loop voltage control with disturbance feedforward by a super-twisting compensation resulted in overall robust output with fast dynamic response. Similar robust, fast dynamic performance was reported in [84] where passivity-based active damping was employed for harmonic suppression.

Generally, the extraction of positive and negative sequences makes the controller more complicated. Therefore, Eslahi et al. [117] proposed a scheme with improved resilience for microgrids. First, the simplified controller avoids the virtual flux approach, whose performance is deteriorated by abnormal grid conditions. Second, it avoids sequence components extraction of grid voltage and current by a novel reference computation scheme in the stationary reference frame. Third, it implements grid-sensorless control by a state/disturbance observer. Nonetheless it is limited by hysteresis-induced variable switching frequency and high power ripples.

D. Circulating Current Suppression

A fast-processing predictive control strategy is proposed in [118] for mitigating circulating current in parallel three-level inverters. To reduce the computational burden, the reference voltage in the $\alpha\beta$ frame is calculated, and the cost function is altered to minimize the voltage error between the reference and feasible voltage vectors. The number of voltage vector candidates is then further reduced to five or six by excluding those that increase circulating current. Similarly, in [119], the current reference tracking problem is transformed into a voltage reference tracking problem, and a virtual vector with an average zero CMV is constructed to achieve neutral point voltage balance and circulating current suppression simultaneously. Ultimately, three vectors are used to synthesize the desired voltage, demonstrating enhanced reference tracking accuracy.

In [120], predictive zero-sequence current control (PZSC ^{2}) is proposed for multiple parallel inverters/rectifiers. The control objectives of current reference tracking and circulating current suppression are achieved by applying a synthesized voltage vector. This synthesized voltage vector is composed of an optimal shrunken voltage vector and a zero voltage vector. The former minimizes the tracking error of the $\alpha\beta$-axis current, while the latter is judiciously chosen to mitigate circulating current. This method operates autonomously, making it well-suited for spatially distributed applications. The control block diagram of the proposed PZSC^2 in [120] for multiple parallel inverters/rectifiers is depicted in Fig. 13. In addition, a centralized carrier-based MPC scheme is presented in [121] for modular parallel converters. The dynamic modeling of circulating current is derived for its trajectory prediction. Based on this, a cost function that minimizes the current tracking error and circulating current for the j th inverter is formulated as

$$J_j = |i_{\alpha j}(k+1) - i^*_{\alpha j}(k+1)|^2 + |i_{\beta j}(k+1) - i^*_{\beta j}(k+1)|^2 + \lambda \sum_{x=1}^{N} |i_{zsx}(k+1) - i^*_{zsx}(k+1)|^2 \quad (16)$$

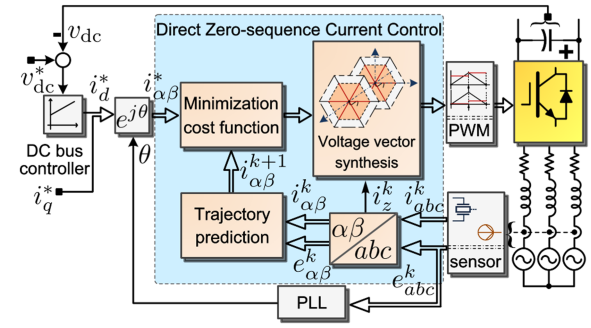

Fig. 13. Diagram of the proposed PZSC^2 in [120] for multiple parallel inverters/rectifiers.

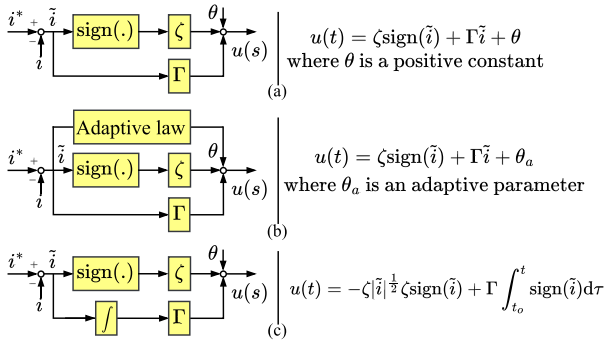

$u(t) = \zeta \text{sign}(\tilde{i}) + \Gamma \tilde{i} + \theta$ where θ is a positive constant

$u(t) = \zeta \text{sign}(\tilde{i}) + \Gamma \tilde{i} + \theta_a$ where θ_a is an adaptive parameter

$u(t) = -\zeta |\tilde{i}|^{\frac{1}{2}} \zeta \text{sign}(\tilde{i}) + \Gamma \int_{t_o}^{t} \text{sign}(\tilde{i}) d\tau$

Fig. 14. SMC schemes [9]. (a) Classical SMC. (b) Adaptive SMC. (c) Second-order SMC.

where $i_{\alpha j}$ and $i_{\beta j}$ denote the jth inverter's current on the $\alpha\beta$ frame, i_{zsx} is the circulating current of the xth inverter ($x \in 1, \ldots N$), and N represents the number of the parallel inverters. Based on this, the unconstrained optimal solution can be obtained by solving the following equation online:

$$\begin{cases} \frac{\partial J_j(v_{\alpha j}, v_{\beta j}, v_{zs1}, \ldots v_{zsN})}{\partial v_{\alpha j}} = 0 \\ \frac{\partial J_j(v_{\alpha j}, v_{\beta j}, v_{zs1}, \ldots v_{zsN})}{\partial v_{\beta j}} = 0 \\ \frac{\partial J_j(v_{\alpha j}, v_{\beta j}, v_{zs1}, \ldots v_{zsN})}{\partial v_{zsj}} = 0 \end{cases} \quad (17)$$

where $v_{\alpha j}$ and $v_{\beta j}$ denote the jth inverter's output voltage on the $\alpha\beta$ frame, while v_{zsx} is the common mode voltage of the xth inverter. In addition, with carrier signals employed, an interleaving mechanism is implemented to reduce the total current ripple. Experimental results show its effectiveness.

E. Other Control Objectives

Control objectives including power sharing, synchronization under weak grid, and grid frequency and voltage support can also be realized with advanced control. Power sharing, an objective better associated with the islanded operation of the microgrid can be improved by PBC, providing a decentralized realization with robustness to line parameters and plug-and-play capability [12].

In order to enhance the transient stability of power synchronization control during grid-fault conditions in weak grids, DNN was proposed for fast detection of synchronization instability in [98]. The scheme, which is robust to data noise, further

TABLE III
TECHNIQUES FOR REDUCING CHATTERING IN SMC [9], [127]

Technique	Advantages and disadvantages
Boundary layer [123]	✓ Low complexity ✓ Constant switching frequency × Trades off control performance
State/disturbance observer [71], [72]	✓ Flexible implementation ✓ Constant switching frequency ✓ Good disturbance rejection × Medium complexity
Second-order SMC† [73]	✓ Finite convergence time ✓ Good robustness to uncertainties × Large disturbances trigger chattering
Hysteresis function [74]	✓ Low complexity × Variable switching frequency × Steady-state error
Fractional-order SMC [75]	✓ Fast dynamics ✓ Good disturbance rejection × High complexity
Intelligent/adaptive SMC [76]	✓ Fast dynamics ✓ Low to medium computational burden × Medium to high complexity

† E.g. STA . × = disadvantage. ✓ = advantage.

ensures that during transients, the phase during the preceding stable operation is stored and utilized to prevent fault-induced loss of synchronism.

Neural network-optimized predictive control for grid frequency support via VSGs is reported in [99] with optimal outcomes for both inductive and resistive line impedances. Fast frequency inertial response can mitigate grid instability in low inertia conditions. Although the popular approach for inertial response requires measuring the ROCOF, the utilizing the dc-link voltage via a novel approach in [122] can improve the stability of the VSC in weak grids.

In the following section, the challenges associated with the advanced control methods and recent related solutions in the literature are reviewed.

VII. CHALLENGES OF ADVANCED CONTROL METHODS AND RECENT SOLUTIONS

This section discusses the challenges and recent solutions for the control methods and applications in Sections V and VI, with particular focus on model-based techniques.

A. Sliding Mode Control

Although SMC has several advantages including simplicity, robustness, and fast dynamic performance, one of its main shortcomings is the chattering effect.

The research literature on SMC for grid-connected power converters documents numerous solutions to chattering through techniques including boundary layer [123], state/disturbance observer [71], second-order SMC [73], hysteresis function [74], and intelligent/adaptive SMC [116] (see Table III). The hysteresis function with a predefined single or double band(s) can restrict the state's trajectory to lessen chattering effects [74]. However, this method is limited by tracking bias and variable switching frequency. The other chattering-reducing techniques generally produce fixed switching frequency.

Boundary layer technique [123] transforms the discontinuity in SMC into a continuous signal within a defined boundary to reduce chattering. State/disturbance observer-based SMC (DO-SMC) employs full-state, disturbance and ESOs to estimate the states, internal and exogenous disturbances in the system. Afterward, the disturbance is rejected by feed-forward control. In order to reduce sensors in a grid-connected modular multilevel converter (MMC), the sliding-mode observer was used for estimating capacitor voltages using the measurements of arm currents and arm voltages [71].

The Luenberger observer was proposed to improve the robustness of current control to grid-frequency and inductance uncertainties, thereby mitigating chattering [72] in the NPC converter. Several techniques are reported to reduce chattering at the expense of disturbance rejection [61]. However, DO-SMC and adaptive SMC [126] are capable of reducing chattering without compromising disturbance rejection.

Second-order SMC methods, e.g., twisting algorithm and super-twisting algorithm (STA), mitigate chattering effects by the integral action that produces continuous control signals from discontinuous functions. STA [73], in particular, has a finite-time convergence and good robustness to uncertainties. Fractional-order SMC combined with passivity control was proposed in [75] to both dampen *LCL*-filter resonances and reduce chattering. Intelligent methods like fuzzy control can adaptively select optimal parameters (optimal fraction-order in [76]) to minimize chattering effects. Fig. 14 illustrates the classical, second-order and adaptive SMC schemes.

Reference-tracking performance of SMC can be improved by the quality of the sliding mode surface. A quasi-integral sliding-mode surface was proposed in [103] to null the mitigate power/voltage steady-state tracking bias for a three-level NPC power converter. Details on the theory and applications of SMC to power converter are provided in [9] and [127].

B. Direct Power Control

The shortfalls of hysteresis-based TB-DPC include variable switching frequency, high power ripple, high current THD, and high sampling frequency. Others include the challenges of implementing effective grid-voltage estimation during disturbances from unideal grid, and robustness to grid parameter uncertainties. State-of-the-art solutions (shown in Fig. 15 and summarized in Table IV) will be discussed in the following.

Space-vector modulated DPC (SVM-DPC) is one of the earliest solutions proposed in [132] to the variable switching frequency limitation of ST-DPC. The classical model has been improved for effective performance under unbalanced and distorted grid voltage conditions [128]; but it has high computational burden due to multiple reference frame transformation. More recently, Gui et al. [77] proposed the grid-voltage modulated DPC (GVM-DPC), an alternative formulation of modulated DPC. GVM-DPC presents the system in the dq frame without using the PLL—it employs a dot product of the grid voltage and the converter voltage in the $\alpha - \beta$ frame, the so-called GVM. This improves the dynamic performance as in the DPC-SVM.

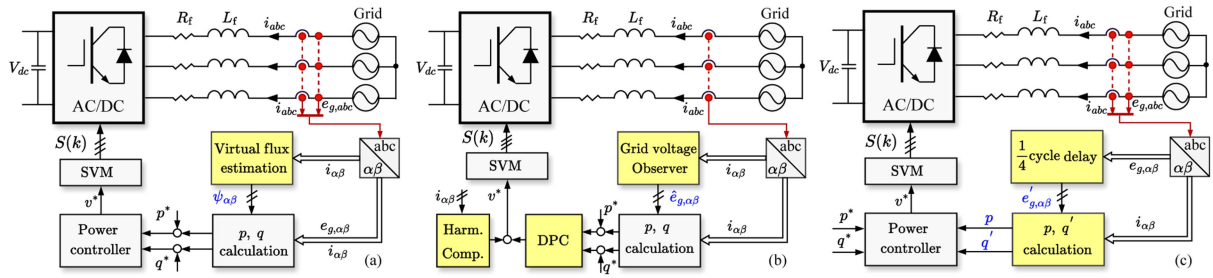

Fig. 15. DPC schemes for grid-connected power converters. (a) DPC with virtual flux estimation. (b) DPC with grid voltage observer and harmonic compensation. (c) DPC with harmonic compensation based on extended instantaneous power theory [124].

TABLE IV
CHALLENGES OF DPC AND RECENT SOLUTIONS

Challenge	Solution
Variable switching frequency	• SVM-DPC [128] • SMC-DPC [125], [129] • Deadbeat PDPC [78]
High power ripple	• MPC-DPC [78], [130] • SVM-DPC [128] • SMC-DPC [125], [129] • Deadbeat PDPC [78]
High sampling frequency	• VF-based estimation [8], [131] • Observer-based estimation [73], [80] • Multi-vector MPC-DPC [78], [130] • Fictive-axis emulation (FAE) [105]
Grid voltage estimation	• VF-based estimation [8], [131] • Observer-based estimation [73], [80]
Sensitivity to grid uncertainties	• GVM-DPC [77] • Stochastic gradient correction [79] • Compensate $L-$deviation [105], [131]

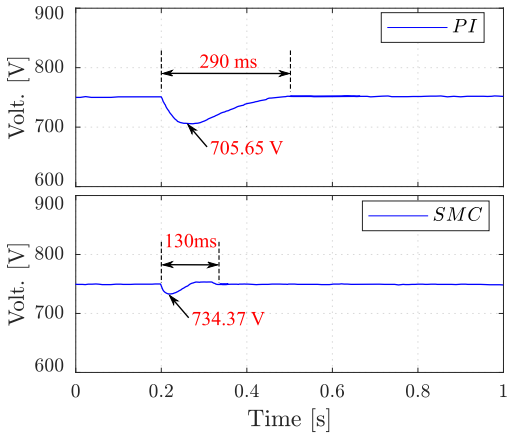

Fig. 16. Experimental results for the transient performance of the DC-link capacitor due to a step change in load [125].

The sliding mode controller-based direct power control (SMC-DPC) was introduced in [129]; it maintains the high dynamic performance of DPC while ensuring constant switching frequency by space-vector modulation. Nonetheless, the chattering characteristics of SMC limit disturbance rejection performance. In [125], the second-order SMC regulates the voltage and instantaneous power tracking, while the disturbance rejection is enhanced by the linear extended state observation of the external disturbance. Results shown in Fig. 16 show that this method reduces settling time by 55%, and voltage undershoot by 65%.

Deadbeat predictive direct power control (PDPC) utilizes the system's model to predict the states, from which the voltage reference (which will be modulated) necessary to drive the output to the reference is computed. Deadbeat PDPC improves over the ST-DPC by its constant switching frequency, lower power ripples and harmonic distortion.

Model-predictive direct power control (MPC-DPC) utilizes the principle of moving horizon control to predict the active and reactive power during each sampling interval. Then, it employs the cost function to choose the optimal switching state that minimizes the error in the power prediction relative to the reference. Further details on MPC are discussed in Section V-E. The classical finite control-set MPC-DPC method applies one voltage vector per sampling interval, but requires high sampling frequency to reduce power ripples. while improvements. The multivector approach applies two or more voltage vectors (with duty cycle optimization) per sampling interval to reduce the steady-state power ripples [130] without increasing sampling frequency; but the tradeoff is an increase in computational burden. Recent improvements to MPC-DPC improve robustness by model-free power prediction from the ultralocal system model, with modifications to compensate for distorted grid conditions [78].

Voltage-sensorless grid voltage estimation for DPC was initially proposed by Noguchi et al. [58], and operates on the duality between the induction motor and the grid-side source with its inductor. The method is limited by erroneous power and voltage estimates at switching instants due to the noisy time derivative of grid current. To overcome this shortcoming, the virtual flux-based power estimation was proposed by Malinowski et al. [133], and thanks to the integral term, avoids the derivative function. Subsequent virtual-flux estimation-related publications have reported diverse ways to compensate the dc-bias introduced by the integrator: the first-order low-pass filter [8], band-pass filter [131], etc. The second family of voltage-sensorless DPC use state observers to estimate the grid voltage. The state observers operate by scaling the error of the estimated quantity with an observer gain with the aim of driving the error to zero. The Luenberger observer, Kalman filter [80] and sliding mode observers [73] are commonly applied to grid voltage estimation. The Kalman filter and sliding mode observer have superior measurement noise

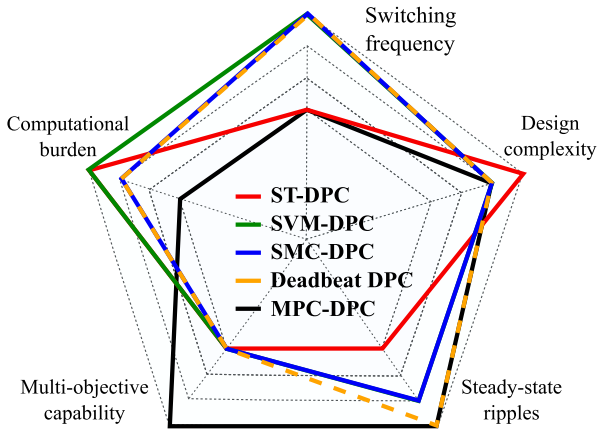

Fig. 17. Features of DPC methods. Performance range: poorest (innermost polygon) to best (outermost polygon). ST-DPC is switching table DPC, SVM-DPC is space vector modulator DPC, SMC is sliding mode control DPC, MPC-DPC is MPC-based DPC.

attenuation than the former, but require higher computational requirements.

Uncertainties in grid parameters, such as the grid voltage, impedance, and frequency, can deteriorate DPC's performance. The mismatch of actual filter/grid inductance from nominal values can limit the performance of MPC-DPC and VF-based control. Therefore, estimating the actual inductance by first computing the VF estimation error, and compensating the inductance deviation can improve robustness to parameter uncertainties [105], [131]. Inductance can also be identified by stochastic gradient correction with the forgetting factor least squares algorithm [79]. Furthermore, GVM-DPC provides a DPC that does not require computation of virtual flux and is robust to distorted grid voltage conditions.

The comparison of the main types of DPC is shown in Fig. 17. Further details on these schemes can be found in [8]. SVM-DPC, SMC-PDC, and deadbeat PDPC guarantee constant programmable switching frequency, overcoming the variable switching frequency limitations of ST-DPC. Also, the high steady-state power ripples and current THD of ST-DPC are significantly reduced by all the other methods. Nonetheless, improved performance over ST-DPC is generally associated with higher computational burden and design complexity.

C. Disturbance-Observer-Based Control

Improving the low/medium-frequency lumped disturbance rejection and convergence rate of ESOs without compromising the suppression of high-frequency measurement noise has been a subject of recent research focus.

The ADRC design of an *LCL*-filtered grid-tied converter can be complicated due to the need for a fourth-order ESO. This hurdle was overcome in [134] by the first-order Pade approximation for the *LCL* filter, ensuring robust control with fast dynamic performance. Therefore, Cao et al. [135] contrived a first-order model for the equivalent *LCCL* filter. This was validated on a 2 kW prototype. The resonance of *LCL* filter was damped by ADRC in [10], where the parameters were determined by root

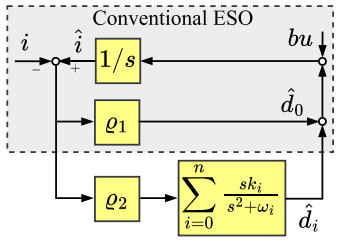

Fig. 18. GIESO with estimation of sinusoidal lumped disturbance $\hat{d}_i$ at harmonic frequency ω_i, where $\omega_0 = 0$ is the fundamental frequency, ϱ_i is the GIESO gain [81].

locus analysis. The closed-loop model was derived with control delay and grid impedance as parameters. A conventional linear ESO facilitated lower sensors than the conventional linear control. All these studies on *LCL* filter require sensing only the grid current, ignoring the impact of the synchronization dynamics. Cheng et al. [136] carried out impedance modeling and Nyquist stability analysis to investigate the sub- and super-synchronous oscillations induced by grid faults, PLL bandwidth and grid impedance in a weak grid condition. From this insight, the stability design was done for the ESO-based control of *LCL* grid-tied converter. In summary, while these studies use the ESO to reduce the number of sensors, further work is required for effective overcurrent and overvoltage protection—which may require additional sensors.

Electrical grids are subjected to varying types of disturbances which can distort the grid voltage magnitude, frequency and phase. Conventional ESOs are best suited for constant or slowly time-varying disturbances, and are unreliable for large, fast-varying periodic disturbances. When the control scheme is implemented in the synchronous reference frame, the constant disturbances (at fundamental-frequency) can be accurately estimated by the ESO; however, harmonic disturbances will be poorly estimated. Guo et al. [81] addressed this problem by proposing a generalized-integrator-ESO (GIESO). GIESO is derived from the conventional ESO whose base pure integrator is capable of reconstructing constant/low-frequency disturbances. GIESO, shown in Fig. 18, further contains multiple generalized integrators (resonant filters), which are tuned to the different frequencies of fast-varying disturbances to be estimated. The effectiveness of GIESO was demonstrated for a controller implemented in the synchronous reference frame, and requires a PLL whose integrity is compromised by harmonics in the distorted grid voltage. The converse of the problem when the control is done in the stationary reference frame was investigated in [82]. The authors proposed the use of resonant ESO to estimate disturbances at the grid frequency, while ensuring adaptiveness to grid frequency changes.

As earlier mentioned, the ease with which ESO can be complemented with other feedback control schemes makes it a popular choice for integration with other nonlinear control methods. Examples include MPC with ESO disturbance rejection [83] and SMC with ESO-based disturbance estimation [73].

D. Passivity-Based Control

The challenges of PBC include the choice of frame of reference for representing both the inverter and network dynamics. Using the local frame makes the network lose its passivity properties, unless the assumption of lossless line is used. Modeling the inverters in the local frame complicates their dynamics. Another issue is the choice of the signals μ, γ in Fig. 11. Inappropriate choice of those can make it difficult to find a controller that satisfy a passivity property. Also, a control design that aims to make an inverter to satisfy a passivity property in Definition 1 can lead to bilinear matrix inequalities, which are nonlinear and are computationally involved [13].

To solve the issues with choice of frame of reference, using the common reference frame allows the network to retain passivity properties, without having to neglect their dynamical behavior and using the lossless assumption [11], [12], [13]. The use of detailed order models makes it easier to identify the appropriate signals for μ, γ [11], [12], [13]. The use of change of variable helps to convert bilinear matrix inequalities into linear matrix inequalities that are easy to solve [11].

Since a microgrid combines VSCs operating in grid-forming and grid-following modes, the stability analysis becomes more complex when classical methods, such as Nyquist criterion, are used. Passivity control with the port-controlled Hamiltonian method combined with PLL-free DPC provides an effective option to guarantee the stability of microgrids with high penetration of VSCs [85]. Passivization of the input admittance by PCC voltage feedforward for the inverter-side current control is a compensation-based method to actively dampen the resonances [86]. Compensation can also be done by grid-side current control with damping injection [87].

Therefore, Xie et al. [88] proposed a general general admittance model that can be flexibly used to control several variables in the *LCL*-filtered grid-connected converter, include converter-side current, grid-side current, and capacitor current/voltage. Also, the passivity controller-parameter design is simplified by this unified approach from zero to the Nyquist frequency. This approach was extended to a the case of current estimation by a Luenberger-observer in [137]. Power-decoupling PBC was introduced in [84], with reported strong disturbance rejection, fast dynamics, high robustness and zero steady-state tracking error. PBC also enhances the performance of other methods like MPC. In [92], a passivity objective term was introduced into the MPC cost function for dynamic damping injection, resulting in lower steady-state error, and improved robustness to endogenous and exogenous disturbances.

E. Model Predictive Control

MPC's challenges with respect to grid-connected converters include complexity of weighting factor tuning, sensitivity to model uncertainties, variable switching frequency, high computational burden, and long prediction horizon. The cost function facilitates the multiobjective constrained control capabilities of MPC with weighting factors that can be difficult to tune optimally. MPC's performance can deteriorate from model inaccuracies arising from parameter mismatches, unmodeled plant dynamics, and measurement noise. FCS-MPC's variable switching frequency produces nondeterministic harmonic spectra; this complicates the design of filters and increases difficulty with compliance with grid-codes' harmonic requirements. The need for optimization during every sampling instant, and long prediction horizons (which increases the accuracy of optimal solution) impose high hardware requirements to manage the increased computational burden. In order to overcome the limitations of conventional FCS-MPC, several solutions have been reported in the literature, and these are discussed in the following.

The challenge of weighting factor tuning is tackled by weighting factor-free cost functions and by optimization of the weighting factor selection. The use of redundant voltage vectors of the power converter [89] and modulated MPC [141] are methods employed to achieve MPC without weighting factor. Also, instead of the time-demanding heuristic tuning of the weighting factor, offline optimization with artificial intelligence, e.g., genetic algorithm [139], has been proposed. Offline tuning can be suboptimal in real-time applications since operating conditions and model uncertainties can change with time. So, online tuning methods (with ANN [140], and non-AI methods [108], [148]) are preferable; but these increase to the computational burden of the controller.

Challenges associated with FCS-MPC's sensitivity to model uncertainties can be mitigated by three main *principles:* prediction error correction, real-time parameter identification, and model-independent (and model-free) state prediction. Methods that utilize the prediction-error-correction principle compensate the state prediction error due to mismatch in the model and actual parameters [90]. Real-time parameter identification with adaptive MPC can also provide some improvement to control performance under parameter mismatch. This is demonstrated via parameter identification with neuro-fuzzy estimator for two-level VSC [149] and modular multilevel converter with virtual flux inductance estimator [131]. However, due to the deviation of the actual parameter from optimal nominal values, the control performance is only slightly improved. Model-independent methods utilize input–output data stored in look-up tables [78] and learning-based artificial intelligence to improve robustness to parameter deviations using ANN, fuzzy logic and RL [143]. Despite their improved robustness to load and parameter uncertainties, the prior three methods have limited immunity to measurement noise.

In order to overcome multiple uncertainties including measurement noise, ultralocal model techniques are gaining increasing research attention. The ultralocal model-based MPC is also called *model-free* predictive control has reduced dependence on the exact model of the system. It uses the so-called *model-free* concept proposed by Fliess and Join [150] to reformulate the plant model in terms of the lumped disturbance, control input, and noisy output as follows [106]:

$$\begin{cases} \dot{x} = & F + \alpha u \\ y = & x + \mathcal{N} \end{cases} \tag{18}$$

where x is the system's state, F represents the total disturbance of the plant, α is a nonzero constant control input gain, $\mathcal{N}$ is

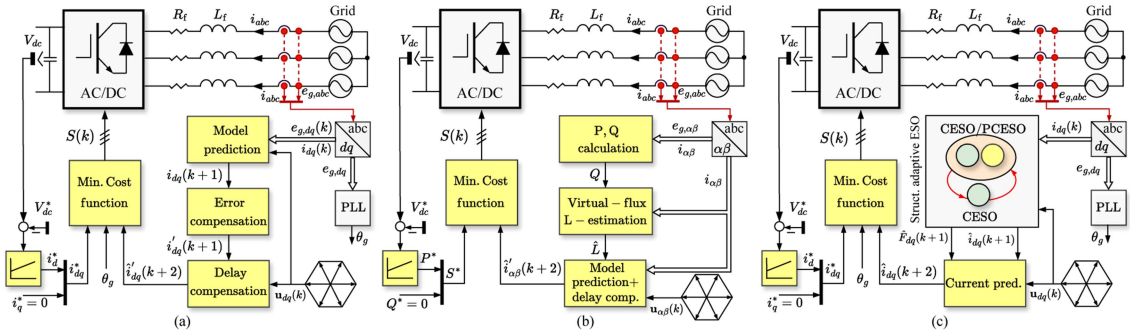

Fig. 19. Robust MPC schemes. (a) MPC with prediction error compensation. (b) MPC with virtual flux-based parameter estimation [131]. (c) Model-free predictive control with structurally adaptive ESO [106].

the measurement noise, and u and y are the control input and measured output respectively. The classical LESO can be used to estimate the lumped disturbance and states. However, due to its limited noise suppression characteristics, recent studies have proposed the use of Kalman filter [151], cascade ESO [83], extended sliding mode observer [152], and hybrid cascade-parallel ESO [91]. Some of these methods are illustrated in Fig. 19.

The problem of FCS-MPC's variable switching frequency can be resolved by hybrid FCS-MPC [144], modulated MPC [138], [145], FCS-MPC with (dis-) continuous modulation [7], and optimal switching sequence MPC (OSS-MPC) [147]. All these schemes produce fixed switching frequencies, improving the converter's output harmonic spectrum for grid-compatibility. For instance, Fig. 21 shows reduced power ripples with modulated generalized predictive power control of a multilevel converter. Karamanakos et al. [7] introduced direct MPC without modulation that ensures 1) one switching action per phase during a sampling interval for continuous modulation and 2) switching of two phases per sampling interval for discontinuous modulation. Hybrid FCS-MPC combines both indirect MPC and direct MPC into the same scheme and can be complicated to implement. Modulated MPC applies dual or multiple switching vectors to the converter during each control interval [146]. OSS-MPC optimizes the switching sequence among the possible converter states [147]. Long-horizon FCS-MPC (LH FCS-MPC) increases the prediction horizon of MPC for improved reference tracking and steady-state performance. Higher predictions impose increase computational burden, which can be alleviated with sphere-decoding algorithms. Nonetheless, LH FCS-MPC has better tracking accuracy than classical FCS-MPC for the closed loop control of high power systems, which operate at low switching frequencies [153]. It should be noted that *deadbeat predictive control*, which also relies on a discrete system model, calculates the necessary control input (usually a voltage reference, which is later modulated) at each sampling instant that will drive the plant's output to a defined reference within a finite control interval of one sampling instant (or more in special cases) [154]. Although deadbeat is usually categorized under *predictive control*, it cannot support multiobjective control, and its control input is an unconstrained solution that might not be optimal for the system's performance.

The computational burden can be decreased by the use of data-driven MPC emulators. For instance, training the ANN model to learn the relationship with input and output relationships of MPC, identical control performance can be achieved with more than 50% reduction in computational burden. The challenge with this approach is the opaque-box approach with makes it difficult to deploy to reliability-critical industrial applications where where physics-based approaches have been the norm. Also, in multistep prediction applications, the sphere-decoding algorithm [94] helps to decrease the classical exponential computational increment associated with long prediction horizons. The discussed challenges and solutions are summarized in Table V.

TABLE V
CHALLENGES OF MPC AND RECENT SOLUTIONS

Challenge	Solution
Weighting factor tuning	• Offline/online optimization [139], [140] • Weighting factor-free [89], [141]
Sensitivity to model uncertainties	• Prediction error correction [90] • Ultralocal model/observer-based [91] • Model-free [142]/ data-based [143] • Parameter identification [131]
Variable switching freq.	• Hybrid FCS-MPC [144] • Modulated MPC [145], [146] • (Dis-) continuous modulation [7] • Optimal switching-sequence MPC [147]
High computational burden	• Data-driven emulator [93]
Long prediction horizon	• Sphere decoding algorithm [94]

VIII. ADVANCES IN DATA-DRIVEN CONTROL OF GRID-CONNECTED VSCs

This section reviews the data-driven methods and their applications to key control objectives in Section II-B.

A. Data-Driven Methods for Grid-Connected VSCs

1) Fuzzy Logic: Due to its advantages, including, intuitiveness, ease of implementation, and ability to handle imprecision and uncertainty, fuzzy logic is a popular research method. In order to minimize chattering in SMC, fuzzy control was applied in [76] and [158] to adaptively select optimal control gains. Furthermore, while observers like disturbance observer and sliding mode observer have been reported to reduce the chattering effect, augmenting the observer's adaptive performance with fuzzy logic produces even superior results [161], [162]. The

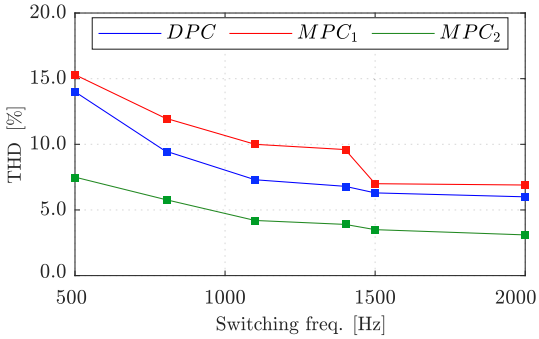

Fig. 20. Experimental results for current THD with respect to switching frequencies [105].

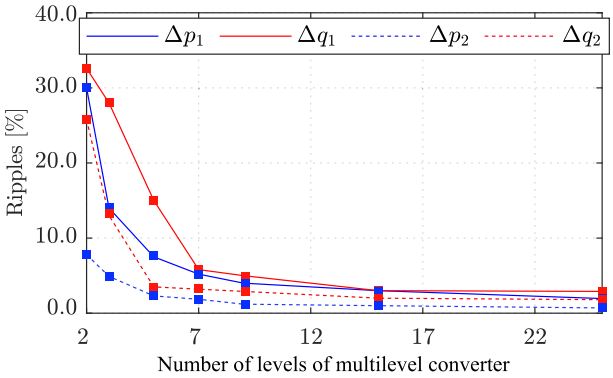

Fig. 21. Experimental results for active and reactive power ripples (Δp and Δq, respectively) for different levels of multilevel converter. Conventional MPC ($\Delta p_1, \Delta q_1$) is compared with generalized predictive power control ($\Delta p_2, \Delta q_2$) in [138].

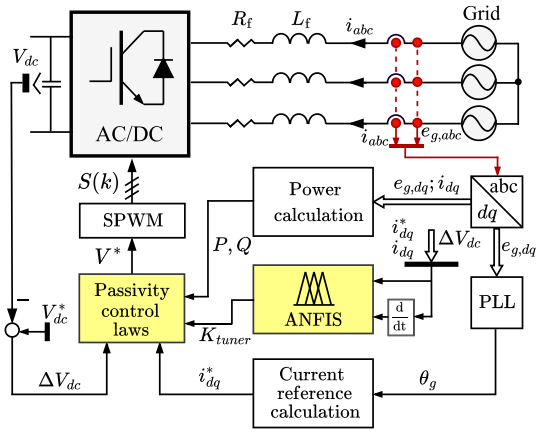

Fig. 22. Passivity-based ANFIS controller [97].

combined use of PSO and fuzzy for the optimal autotuning of proportional–integral controller gains for active and reactive power control was reported in [107] with robust, low-ripple steady-state results, and faster transient convergence than the classical methods. A type-2 fuzzy logic controller was applied in [95] for the high-performance control of a nine-level packed E-cell inverter. In particular, this controller eliminates the error arising from model uncertainties in ESO operation, ensuring accurate steady-state reference current tracking. Nonetheless, these methods inherit limitations of fuzzy logic, requiring expert knowledge of the system for optimal design. Also, the fuzzy rules are not adaptive to changing system conditions and require re-tuning; meanwhile, fuzzy logic becomes more complicated to implement as the rules increase.

2) Adaptive Neuro-Fuzzy Inference System: ANFIS method merges the human-like reasoning of fuzzy systems with the learning capabilities of neural networks, resulting in fuzzy rules that adapt to new data, and can improve over time. Damping injection based on passivity principle can improve the stability of grid-tied converters. Therefore, Mehrasa et al. [97] utilized the adaptive neuro-fuzzy controller to regulate the damping coefficients required to maintain stability over a wide operational range of the converter (see Fig. 22). Also, in [110], the ANFIS controller utilized active and reactive power errors to determine the reference voltage for FRT control. Shortcomings of ANFIS are its computational and resource intensiveness; also, the tuning process is more demanding for both fuzzy rules and neural network parameters.

3) Neural Networks: ANN is excellent at managing complex nonlinear relationships in data, and is flexible. For these reasons, it is one of the most popular data-driven methods applied to grid-connected VSCs. There are three main applications: optimal parameter tuning, stability enhancement, and emulation of other advanced controllers. Mehrasa et al. [96] employed ANN to optimize the online parameter tuning for input–output feedback linearization control of packed E-cell converter. DNN was applied in [98] for online stability parameter tuning to ensure transient stability of power synchronization in weak grids.

Controller emulation is one of the most common applications of neural networks in control of grid-tied converters. A hybrid ANN-MPC scheme optimizes the transient performance of a VSG by using ANN model to predict the frequency during the sampling interval of the model-predictive controller. [99]. The shortcoming of this method is its inability to adapt to conditions of parameter changes. ANN was further employed for optimal weighting factor tuning MPC [102], [160], alleviating the conventional time-taking trial and error procedure. The advanced features of other neural networks have also been harnessed: for instance RNN which has memory of previous data and is useful for sequential data of variable length. RNN was applied as a surrogate of MPC in [165] for the current control of a grid-tied multilevel converter. However, RNN has higher training complexity because it involves backpropagation through time, and has vanishing and exploding gradients. Also, the general limitation of ANN and RNN include the need for large amounts of training data to perform effectively; acquiring these data experimentally can be expensive. Also, they are considered *opaque-box* approaches due to difficulty in understanding the internal workings.

4) Physics-Informed Neural Networks (PI-NN): PI-NN integrates known physical laws into the learning process, improving model reliability. Thus, it requires less data for effective generalization—implying faster training time—and the models are more interpretable. An efficient technique for oscillation

TABLE VI
DATA-DRIVEN CONTROL OF GRID-CONNECTED AC/DC POWER CONVERTERS

Objective	Data-driven method	Nonlinear technique	Application	Features
Stability enhancement	DNN [98]	–	2L-VSC	Enhances stability of power synchronization control.
	Fuzzy logic [95]	–	2L-VSC	Enhances performance of extended state observer.
	PI-NN [100]	–	2L-VSC	Dampens oscillations.
	Neuro-fuzzy [97]	Passivity	PEC9	Regulates damping coefficients.
Optimal control	RNN [155]	–	2L-VSC	Low sampling rate and switching frequency.
	ANN [156]	–	*LCL*-filtered VSC	–
	PI-NN [157]	–	2L-VSC	Physics-informed AI with low-cost implementation.
	Bayesian network [101]	MPC	Distribution n/w	Robust control with online control law update.
	ANN [99]	MPC	VSG	Optimizes the transient performance of VSG.
	Neuro-fuzzy [110]	DPC	DFIG	P, Q comparator for reference voltage.
	Fuzzy [76]	FONT-SMC	VSC	Chattering mitigation.
	Fuzzy [158]	SMC	VSC for PV	Chattering mitigation.
Optimal parameter design	Fuzzy-Q learning [159]	–	PEC9	Adaptive controller coefficients.
	ANN [96]	–	PEC9	
	PSO + ANN [102]	MPC	VSC	Weighting factor tuning.
	ANN [160]	MPC	3L-NPC	
Disturbance rejection	RL [20]	–	HESS	Decentralized scheme with plug and play capability.
	Fuzzy [161]	SMC + DO	1-Ph PV inverter	Disturbance rejection with minimal chattering.
	Fuzzy [162]	SMC + SMO	VSC	
Controller emulation	ANN (two kinds) [163]	MPC	MMC	NN regression has better performance and lower computational burden than pattern recognition.
	Time-delay NN [164]	MPC	3L-NPC	
	RNN [165]	MPC	VSC	Emulates MPC.
Parameter identification	PI-NN [166]	–	MMC	Online impedance identification.

FONT-SMC is fractional-order nonsingular terminal sliding-mode controller, DO is disturbance observer, SMO is sliding mode observer, PSO is particle swarm optimization, PEC9 is nine-level packed E-cell inverter

dampening of grid-tied power converters using PI-NN was proposed in [100]. In particular, changes in grid current or voltage are quickly dampened in the dc-link capacitor voltage, improving robustness. Also, PI-NN was employed for impedance identification of grid-tied MMC in [166], improving the reliability and robustness of the controller.

5) Bayesian Network: Bayesian network provides robust probabilistic reasoning, handling uncertainty effectively. Wang et al. [101] introduced a dynamic Bayesian network predictor for MPC. It can enhance optimal control by online learning of the parameters, further improving the accuracy of the model prediction for optimal feedback control. Meanwhile it provides further robustness to stochastic uncertainties.

6) Reinforcement Learning: RL's capabilities for learning optimal policies through interaction with the environment and sequential decision-making make it suitable for dynamic and complex environments. Disturbance rejection was implemented in [20] for a hybrid energy storage system. The scheme uses RL to learn the optimal approach to disturbance estimation and smoothen out the impacts of changes from charging to discharging mode, and the variations of renewable intermittency. RL's shortcomings are requirements of large amounts of data and computationally intensive/time-consuming training process.

7) Particle Swarm Optimization: PSO is simple to understand and implement, is effective for optimizing complex, nonlinear problems, and does not require gradient information—making it versatile. It is widely applied to optimization problems: Mardani et al. [102] employed PSO for the optimal selection of weighting factors for MPC. PSO was first used for offline tuning, and ANN was deployed for online tuning. PSO was also combined with a fuzzy controller for optimal autotuning of proportional–integral controller gains [107]. The resulting active and reactive power control was robust, had low-ripple steady-state results and faster transient convergence than the classical methods.

B. Data-Driven Solutions to Key Control Objectives

The data-driven control techniques introduced in Section V-F have been applied to several other control objectives than were covered in Section VI. The literature reports applications to stability enhancement, optimal control, disturbance rejection, parameter design, and controller emulation. In many cases, the data-driven methods are also combined with other nonlinear model-based control techniques for enhanced performance. These applications are summarized in Table VI and further elucidated in this section.

1) Stability Enhancement: The high penetration of grid-interfaced distributed energy resources introduces unique challenges for the stability of grid-connected converters. In particular, a weak grid (i.e., power grid with low short-circuit ratio) like microgrids can cause unsteady voltage/frequency at the power converter's terminal, ultimately leading to instability. Since the inverter's stability is determined by both the grid's resistance-to-inductance ratio and the grid inductance, stability can be passively improved by increasing the grid-side *LCL* filter, passive damping resistance, and by the active modification of controller parameters, and time delay [167]. Furthermore, grid faults introduce perturbations that destabilize the synchronization of the converter to the grid. Therefore, machine learning is beneficial for robust early detection of synchronization instability of power synchronization control. After detection, phase freezing can be applied to preserve synchronism during grid faults [98] using DNN. Adaptive neuro-fuzzy system was

TABLE VII
PERFORMANCE COMPARISON OF ADVANCED CONTROL METHODS

Method	Comp. burden	Sw. freq.	Complexity	Robustness	Dynamic perf.	Disturb. Rejection	Multiobj. control
SMC	Low	Low	Low	High	High	Medium[1]	Low
DPC	Low	High[2]	Low	Low[3]	High	Medium	Low[4]
DOBC	Low	Low	Low	High	High	High	Low
Passivity-based	Medium	Low	Medium	High	High	High	Medium
MPC	High[5]	High[6]	Medium	Low[7]	High	High	High
Data-driven control	Low	Low	High	High	High	High	High
Classical PI-PWM	Low	Low	Low	Low	Low	Low	Low

Performance range: low, medium, and high. The following recent variant-techniques overcome shortcomings with improved performances: SMC[1]: Adaptive SMC, disturbance-observer-SMC, 2nd-order SMC. DPC[2]: Space vector modulation-DPC, SMC-DPC, deadbeat predictive DPC. DPC[3]: Grid voltage modulation-DPC, DPC with identification. DPC[4]: MPC-DPC. MPC[5]: Neural network-MPC. MPC[6]: modulated MPC, optimal switching sequence-MPC, continuous control-set-MPC. MPC[7]: model-free MPC, disturbance-observer-MPC.

proposed in [95] to adapt the passivity-derived damping coefficients and maintain stability of the nine-level packed E-cell inverter during transients. Also a PI-NN has lower-data requirement and faster training time than conventional ANN models—a more efficient technique for oscillation dampening of grid-tied power converters [100].

2) Optimal Control and Parameter Selection: Data-driven methods can also produce more optimal control performance than model-based techniques. RNN-based control of two-level VSC enables lower sampling rate and switching frequency than model-based approaches [155]. A dynamic Bayesian network predictor for an MPC scheme can enhance optimal control by online learning of the parameters, further improving the accuracy of the model prediction for optimal feedback control [101]. A related hybrid ANN-MPC scheme optimizes the transient performance of a VSG too [99]. Furthermore, the performance of SMC is enhanced as fuzzy control is applied to adaptively select optimal control parameters to mitigate chattering [76], [158]. These methods also facilitate optimal weighting factor tuning for MPC [102], [160]. Mardani et al. [102] used a dual PSO and ANN scheme for the optimal selection of weighting factors; PSO was first used for offline tuning, and ANN was deployed for online tuning.

3) Other Control Objectives: RL-based disturbance rejection was implemented in [20] for a hybrid ESS to smoothen out the impacts of change from charging to discharging mode, and the variations of renewable intermittency. Fuzzy-enhanced SMC with disturbance-observers also provide an effective way to achieve minimal chattering in SMC without compromising the disturbance rejection performance [161], [162]. Since MPC is characterized by high computational burden, ANN emulators which are trained by the normal MPC controller can significantly decrease the computational burden for multilevel grid-tied converters while maintaining the high-dynamic performance of the traditional MPC scheme [163], [164], [165]. Also, data-driven parameter identification is reported to improve robustness, e.g., MMC impedance identification by physics-informed ANN [166], and VSC *LC*-filter parameter identification by a neuro-fuzzy estimator [149].

IX. OVERALL EVALUATION AND FUTURE TRENDS

This section presents the comparative evaluation and future trends on the methods reviewed in this study. The advanced control methods are compared with respect to their advantages/disadvantages, and relative performances based on computational burden, switching frequency, complexity, robustness, dynamic performance, disturbance rejection, and multiobjective control.

A. Overall Evaluation

The performance comparison of the reviewed control methods is depicted in Table VII. All methods apart from MPC have low computational burden akin to the classical linear control. Artificial neural-network emulation of MPC (ANN-MPC) [69], for instance, has been proposed to reduce the computational burden of MPC. The switching frequencies of DPC and MPC, in their classical forms, are variable, but space-vector modulated DPC and modulated MPC, respectively, mitigate this shortcoming (in addition to other methods listed in Table VII). The complexity of the methods varies: SMC, DPC, and DOBC are easiest to design and implement, while MPC, passivity-control and data-driven control are more complex to design and/or implement.

Considering robustness, DPC and FCS-MPC are the most sensitive to model uncertainties; but solutions like SVM-DPC and model-free MPC, respectively, alleviate this problem. SMC's chattering problem and associated solutions generally tradeoff its disturbance rejection capability; but this weakness is overcome with second-order SMC, adaptive SMC and disturbance-observer-SMC. Multiobjective control is achievable with PBC, data-driven control and MPC. PBC is capable of controlling for energy efficiency and stability. Artificial intelligence leverages machine learning to adapt and optimize the control of complex systems. However, MPC also gives added advantages of constrained optimization during the online computation of control inputs. In summary, each control strategy has its advantages and drawbacks. Therefore, the most appropriate for any application would be the one with the best balance between complexity, performance and cost.

B. Future Trends and Research Opportunities

Expected trends in the advanced control of grid-tied converters for microgrids include data-driven fault-tolerant control, cyber-security, synchronization in weak grids, etc.

a) Data-driven fault-tolerant control: Grid-connected microgrids can be subjected to different kinds of faults, namely:

TABLE VIII
DATA-DRIVEN FAULT MANAGEMENT TECHNIQUES FOR GRID-CONNECTED MICROGRIDS

	Grid-FRT Control	Power Converter Fault-Tolerant Control
Objective	Keep the system connected to the grid during grid faults	Maintain converter operation after internal faults
Type of Fault	External (grid voltage sags, frequency issues, etc.)	Internal (switch, sensor, control failures)
Control Strategy	Reactive power compensation, current limiting, PLL adjustments	Reconfiguration, redundancy, adaptive control, switch bypass
Time Horizon	Short-term (milliseconds to seconds)	Longer-term operation in degraded mode
System Focus	Grid interaction and grid stability	Internal reliability of the converter

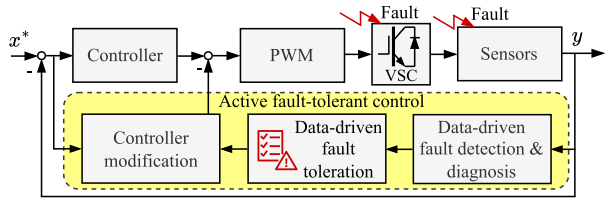

Fig. 23. Generalized plant/sensor fault detection, diagnosis and fault-tolerant control of VSCs.

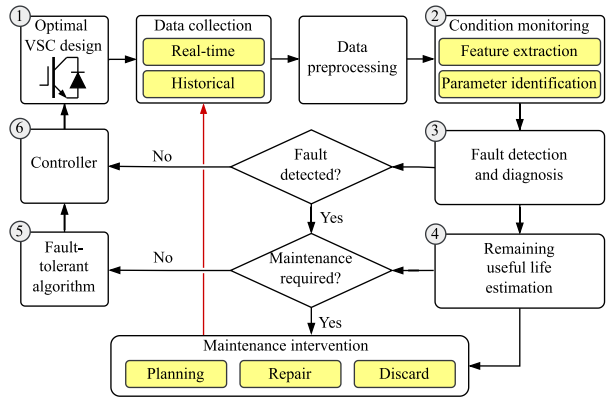

Fig. 24. Workflow of data-driven control and predictive maintenance of reliable grid-connected power converters.

external grid faults (voltage dips, frequency deviations, and grid disturbances) and internal power converter faults (of power semiconductor switches, sensor faults, and control system failures). Grid faults can be mitigated by diverse *grid-FRT* solutions earlier discussed. However, converter faults can be mitigated by *fault-tolerant* control strategies, to enhance the reliability and operational continuity of the system. Table VIII summarizes fault-management techniques in grid-connected microgrids. Although several techniques for data-driven grid-FRT have been reported in the literature (as earlier discussed), studies on data-driven fault-tolerant control solutions for grid-connected power converters remain scant.

Fault-tolerant control comprises both active and passive methods. Active fault-tolerant control incorporates distinctive schemes for fault detection/diagnosis, fault accommodation and controller reconfiguration for effective operation in the fault-tolerant mode. However, passive methods only feature robust controllers with limited fault-management capacity. For instance, consider Fig. 23 which shows a data-based scheme for active fault-tolerant control.

The workflow for the data-driven control and predictive maintenance of grid-connected converters is shown in Fig. 24. It highlights six main applications of data-driven methods, namely, optimal design of highly reliable VSC, condition monitoring, fault detection and diagnosis, remaining useful life estimation, fault-tolerant control, and the optimal control of a grid-connected VSC.

Fault-tolerant performance is ensured by three techniques: hardware design, appropriate control, and a hybrid of both hardware and control strategies. Data-driven methods can be applied to aid the design of fault-tolerant circuits driven by the three principles of device redundancy, phase redundancy and open/short-circuit state-redundancy [168]. Furthermore, the optimal filter size that ensures lifetime reliability can be determined through AI-based multiobjective optimization from simulation or experimental data [169].

Condition monitoring covers the techniques to identify system parameters and extract features that are useful to monitor the health of the system, whether healthy or faulty. Least-squares optimization and machine-learning models are some of the reported methods for parameter identification and feature extraction [170].

Fault detection determines system parameter deviation from healthy conditions, revealing existing, or imminent failures. Machine learning methods are useful for revealing degradation that precedes catastrophic system failure, informing predictive maintenance interventions. Also, fault diagnosis identifies the exact fault to either prevent or reduce equipment downtime (for maintenance). The kind of dataset collected–labeled, unlabeled, or partially labeled–determines if supervised, or unsupervised AI techniques will be employed. Remaining useful life estimation is done with statistical or machine learning models to predict the time left for degradation to reach a failure threshold [170]. The outcome of this analysis informs planning for repair and/or replacement of the equipment.

In summary, further research investigations are necessary to develop effective data-driven fault-tolerant techniques to improve the life-time reliability of grid-connected microgrids.

b) Cyber-security: Grid-connected microgrids are part of larger smart grid system that now relies on data collection for both analytics and system-wide optimization. This requires power converters to operate in a cyber-physical domain that is more vulnerable to cyber-attacks. Remote monitoring and communication systems facilitate numerous advanced control possibilities in microgrids with high penetration of power electronics. However, these high-performance features also make the system vulnerable to security breaches. Cyber-attacks on microgrids usually aim to compromise data availability, integrity, and confidentiality, e.g., denial of service (DOS), false-data injection attack (FDIA), and man-in-the-middle (MITM) attack. DOS

aims to disrupt services by overwhelming the target system with traffic or requests. In MITM, the attacker intercepts, eavesdrops, alters, and steals data from a communication channel. FDIA compromises the integrity of data being transmitted, stored, or processed to deceive systems or users. Grid-tied microgrids are vulnerable to these attacks through sensor attacks on voltage sensors to compromise integrity of measurements, attacks on protection systems to cause system shut down, and attacks on frequency control to cause transient instability, etc [171]. These can lead to undesirable impacts including poor voltage profile control, equipment overload and wear out, and unnecessary tripping of protection relays.

Improved cyber-security can be integrated into the reviewed advanced control methods through low-cost anomaly/intrusion detection, and attack mitigation strategies. For instance, using physics-based residual approach, the residual between the estimated and received data can be compared with a threshold through specialized statistical algorithms [172]. Dynamic watermarking is an alternative method, where a confidential signal is superimposed on the control input (watermark), and an alarm is raised if the data received from the sensors lacks the correct component of the secret watermark [173]. Further research is necessary to develop cyber-secure techniques with minimum financial implication on the grid-tied microgrid.

c) Communication network challenges: Communication networks are mainly necessary at the secondary control hierarchy of microgrids. Ideally, the communication channel should facilitate real-time transmission of data between agents of the microgrid. However, this comes with practical constraints relating to cost of deployment. Therefore, a tradeoff of performance usually results. For more resilient scalable operation of the microgrid, distributed control schemes are growing in popularity since they can operate effectively with lower cost communication bandwidth. This approach also makes the system more susceptible to uncertainties in reliability, latency requirements, packet errors, variable link capacity, harsh environmental conditions, and resource constraints. Therefore, more effective solutions are needed to guarantee effective microgrid control performance despite these communication constraints.

d) Grid-interactive electric-mobility: The techniques discussed above are specifically for stationary grid-tied power converters. However, as the penetration of electric vehicles (EV) increases, their bidirectional vehicle-to-grid functionalities will become essential for grid support. Therefore, the extension of these techniques to onboard and stationary EV infrastructure will become prevalent in the near future. Also, EV fast-charging stations have unique characteristics, that lead to power quality challenges, including high charging power and pulsating load due to high power requirements within a short charging time. Therefore, research is needed for solutions, especially in respect of grid voltage fluctuations, harmonic stability and harmonic emissions.

e) Hybrid controllers: The study indicates that each advanced control technique has its strengths and weaknesses. However, an emerging trend in the literature involves merging controllers with complementary characteristics: DPC with MPC, and DOBC with SMC/MPC, etc. Also, the growth of AI outside of the power electronics field has created effective tools that can be applied to improve different aspects of power converter control. Advanced control design can be eased by utilizing AI for adaptive optimal parameter selection. Furthermore, the learning capabilities of AI can be employed to further reduce the computational burden and hardware cost of methods like MPC without compromising performance.

f) Optimality and efficiency: The methods discussed in this review are mainly time-triggered control approaches, which continue to consume computational resources despite operational conditions remaining consistent over a long sampling interval. However, in order to improve computational and energy efficiency, event-triggered techniques will be beneficial. Also, the recent advancements in MPC and its variants demonstrate their benefits in facilitating implementation. However, simplifying the optimization problem—by reformulating the cost function or restricting the feasible control set—can impact the optimality and, consequently, reduce system performance. A common approach simplifies by treating paralleled power converters independently and solving the optimization problems of current tracking and ZSCC suppression in sequence [120], [174]. These methods lead to suboptimal solutions, which degrade performance in both steady states and during transients. To address these limitations, it is crucial to properly and formally formulate the FCS-MPC problem. In addition, developing a computationally efficient algorithm that ensures optimal solutions is essential for overcoming these challenges.

g) VSCs in weak grids: It has been mentioned that grid-forming converters do not manifest the side-band oscillations associated with grid-following converters in weak grids. Nonetheless, research efforts are still required to establish the stability requirements for grid-forming converters. In addition, further efforts are necessary to establish comprehensive analytical techniques for designing the integration of multiple VSCs into the grid.

X. Conclusion

The grid-integration of renewable microgrids through advanced nonlinear controlled power electronic converters has strong potential for improved performance and reduced complexity in multiobjective and multitimescale control. All methods apart from MPC have low computational burden like the classical linear control. The switching frequency of DPC and MPC can be variable. The complexity of the methods varies: SMC, DPC and DOBC are easiest to design and implement, while MPC, passivity-control and data-driven control are more complex to design and/or implement. DPC and FCS-MPC are the most sensitive to model uncertainties. Multiobjective control is achievable with both MPC and PBC; MPC gives the added advantage of constrained optimization during the computation of control inputs. The trend of related research shows significant opportunities for improvements through optimality, fault-tolerant control, efficiency, cyber-security, robustness to communication network uncertainties, grid-interactive mobility applications, and improved analytical design for large-scale grid-integration of converters.

REFERENCES

[1] J. B. Rawlings, "Tutorial overview of model predictive control," *IEEE Control Syst. Mag.*, vol. 20, no. 3, pp. 38–52, Jun. 2000.

[2] T. Dragičević, S. Vazquez, and P. Wheeler, "Advanced control methods for power converters in DG systems and microgrids," *IEEE Trans. Ind. Electron.*, vol. 68, no. 7, pp. 5847–5862, Jul. 2021.

[3] Y. Huang and W. Xue, "Active disturbance rejection control: Methodology and theoretical analysis," *ISA Trans.*, vol. 53, no. 4, pp. 963–976, 2014.

[4] N. Oikonomou, C. Gutscher, P. Karamanakos, F. D. Kieferndorf, and T. Geyer, "Model predictive pulse pattern control for the five-level active neutral-point-clamped inverter," *IEEE Trans. Ind. Appl.*, vol. 49, no. 6, pp. 2583–2592, Nov./Dec. 2013.

[5] M. A. Awal, H. Yu, H. Tu, S. M. Lukic, and I. Husain, "Hierarchical control for virtual oscillator based grid-connected and islanded microgrids," *IEEE Trans. Power Electron.*, vol. 35, no. 1, pp. 988–1001, Jan. 2020.

[6] A. Elnady, A. Noureldin, and A. A. Adam, "Improved synergetic current control for grid-connected microgrids and distributed generation systems," *J. Modern Power Syst. Clean Energy*, vol. 10, no. 5, pp. 1302–1313, 2022.

[7] P. Karamanakos, M. Nahalparvari, and T. Geyer, "Fixed switching frequency direct model predictive control with continuous and discontinuous modulation for grid-tied converters with LCL filters," *IEEE Trans. Control Syst. Technol.*, vol. 29, no. 4, pp. 1503–1518, Jul. 2021.

[8] S. Yan, Y. Yang, S. Y. Hui, and F. Blaabjerg, "A review on direct power control of pulsewidth modulation converters," *IEEE Trans. Power Electron.*, vol. 36, no. 10, pp. 11984–12007, Oct. 2021.

[9] L. Wu, J. Liu, S. Vazquez, and S. K. Mazumder, "Sliding mode control in power converters and drives: A review," *IEEE/CAA J. Automatica Sinica*, vol. 9, no. 3, pp. 392–406, Mar. 2022.

[10] W. Ma, Y. Guan, B. Zhang, and L. Wu, "Active disturbance rejection control based single current feedback resonance damping strategy for LCL-type grid-connected inverter," *IEEE Trans. Energy Convers.*, vol. 36, no. 1, pp. 48–62, Mar. 2021.

[11] P. Nahata and G. Ferrari-Treeate, "Passivity-based voltage and frequency stabilization in ac microgrids," in *Proc. 18th Eur. Control Conf.*, 2019, pp. 1890–1895.

[12] Y. Ojo, J. D. Watson, K. Laib, and I. Lestas, "A distributed scheme for voltage and frequency control and power sharing in inverter-based microgrids," *IEEE Trans. Control Syst. Technol.*, vol. 31, no. 4, pp. 1679–1691, Jul. 2023.

[13] J. D. Watson, Y. Ojo, K. Laib, and I. Lestas, "A scalable control design for grid-forming inverters in microgrids," *IEEE Trans. Smart Grid*, vol. 12, no. 6, pp. 4726–4739, Nov. 2021.

[14] J. Hu, Y. Shan, K. W. Cheng, and S. Islam, "Overview of power converter control in microgrids—challenges, advances, and future trends," *IEEE Trans. Power Electron.*, vol. 37, no. 8, pp. 9907–9922, Aug. 2022.

[15] E. Mohammadi, M. Alizadeh, M. Asgarimoghaddam, X. Wang, and M. G. Simões, "A review on application of artificial intelligence techniques in microgrids," *IEEE J. Emerg. Sel. Topics Ind. Electron.*, vol. 3, no. 4, pp. 878–890, Oct. 2022.

[16] C. Wu and F. Blaabjerg, "Advanced control of power electronic systems—An overview of methods," in *Control of Power Electronic Converters and Systems*, vol. 3. Elsevier, 2021, pp. 1–33.

[17] J. M. Guerrero, M. Chandorkar, T. L. Lee, and P. C. Loh, "Advanced control architectures for intelligent microgrids Part I: Decentralized and hierarchical control," *IEEE Trans. Ind. Electron.*, vol. 60, no. 4, pp. 1254–1262, Apr. 2013.

[18] Y. Yang, P. Enjeti, F. Blaabjerg, and H. Wang, "Wide-scale adoption of photovoltaic energy: Grid code modifications are explored in the distribution grid," *IEEE Ind. Appl. Mag.*, vol. 21, no. 5, pp. 21–31, Sep./Oct. 2015.

[19] IEEE, "IEEE standard for interconnection and interoperability of distributed energy resources with associated electric power systems interfaces," IEEE Std 1547-2018 (Revision of IEEE Std 1547-2003), 2018.

[20] J. Duan, Z. Yi, D. Shi, C. Lin, X. Lu, and Z. Wang, "Reinforcement-learning-based optimal control of hybrid energy storage systems in hybrid AC–DC microgrids," *IEEE Trans. Ind. Informat.*, vol. 15, no. 9, pp. 5355–5364, Sep. 2019.

[21] O. Babayomi, Y. Li, and Z. Zhang, "Distributed consensus-based reactive power sharing in microgrids: A predictive virtual capacitance control technique," *Int. J. Elect. Power Energy Syst.*, vol. 141, 2022, Art. no. 108139.

[22] Z. Quan and Y. W. Li, "A three-level space vector modulation scheme for paralleled converters to reduce circulating current and common-mode voltage," *IEEE Trans. Power Electron.*, vol. 32, no. 1, pp. 703–714, Jan. 2017.

[23] A. Tcai, Y. Kwon, S. Pugliese, and M. Liserre, "Reduction of the circulating current among parallel NPC inverters," *IEEE Trans. Power Electron.*, vol. 36, no. 11, pp. 12504–12514, Nov. 2021.

[24] K. Sun, X. Lin, Y. Li, Y. Gao, and L. Zhang, "Improved modulation mechanism of parallel-operated t-type three-level PWM rectifiers for neutral-point potential balancing and circulating current suppression," *IEEE Trans. Power Electron.*, vol. 33, no. 9, pp. 7466–7479, Sep. 2018.

[25] H. Xu, L. Xu, C. Li, K. Wang, Z. Zheng, and Y. Li, "Improved interleaved discontinuous PWM for zero-sequence circulating current reduction in three-phase paralleled converters," *IEEE Trans. Ind. Electron.*, vol. 68, no. 9, pp. 8676–8686, Sep. 2021.

[26] D. Razmi, O. Babayomi, A. Davari, T. Rahimi, Y. Miao, and Z. Zhang, "Review of model predictive control of distributed energy resources in microgrids," *Symmetry*, vol. 14, no. 8, 2022, Art. no. 1735.

[27] L. Harnefors, J. Kukkola, M. Routimo, M. Hinkkanen, and X. Wang, "A universal controller for grid-connected voltage-source converters," *IEEE Trans. Emerg. Sel. Topics Power Electron.*, vol. 9, no. 5, pp. 5761–5770, Oct. 2021.

[28] O. Babayomi, Z. Li, and Z. Zhang, "Distributed secondary frequency and voltage control of parallel-connected VSCS in microgrids: A predictive VSG-based solution," *CPSS Trans. Power Electron. Appl.*, vol. 5, pp. 342–351, 2020.

[29] O. Babayomi, Z. Li, Z. Zhang, Y. Sun, T. Dragicevic, and J. Rodriguez, "The role of model predictive control in microgrid power quality - A survey," in *Proc. IEEE 11th Int. Symp. Power Electron. Distrib. Gener. Syst.*, 2020, pp. 340–345.

[30] X. Wang, M. G. Taul, H. Wu, Y. Liao, F. Blaabjerg, and L. Harnefors, "Grid-synchronization stability of converter-based resources—An overview," *IEEE Open J. Ind. Appl.*, vol. 1, pp. 115–134, 2020.

[31] Y. Gui, F. Blaabjerg, X. Wang, J. D. Bendtsen, D. Yang, and J. Stoustrup, "Improved DC-link voltage regulation strategy for grid-connected converters," *IEEE Trans. Ind. Electron.*, vol. 68, no. 6, pp. 4977–4987, Jun. 2021.

[32] Q. Liu, T. Caldognetto, and S. Buso, "Stability analysis and auto-tuning of interlinking converters connected to weak grids," *IEEE Trans. Power Electron.*, vol. 34, no. 10, pp. 9435–9446, Oct. 2019.

[33] X. Zhang, D. Xia, Z. Fu, G. Wang, and D. Xu, "An improved feedforward control method considering PLL dynamics to improve weak grid stability of grid-connected inverters," *IEEE Trans. Ind. Appl.*, vol. 54, no. 5, pp. 5143–5151, Sep./Oct. 2018.

[34] X. Zhang, S. Fu, W. Chen, N. Zhao, G. Wang, and D. Xu, "A symmetrical control method for grid-connected converters to suppress the frequency coupling under weak grid conditions," *IEEE Trans. Power Electron.*, vol. 35, no. 12, pp. 13488–13499, Dec. 2020.

[35] B. Wen, D. Boroyevich, R. Burgos, P. Mattavelli, and Z. Shen, "Analysis of D-Q small-signal impedance of grid-tied inverters," *IEEE Trans. Power Electron.*, vol. 31, no. 1, pp. 675–687, Jan. 2016.

[36] D. Yang, X. Wang, F. Liu, K. Xin, Y. Liu, and F. Blaabjerg, "Symmetrical PLL for SISO impedance modeling and enhanced stability in weak grids," *IEEE Trans. Power Electron.*, vol. 35, no. 2, pp. 1473–1483, Feb. 2020.

[37] S. Wang, Z. Liu, J. Liu, D. Boroyevich, and R. Burgos, "Small-signal modeling and stability prediction of parallel droop-controlled inverters based on terminal characteristics of individual inverters," *IEEE Trans. Power Electron.*, vol. 35, no. 1, pp. 1045–1063, Jan. 2020.

[38] Y. Tao, Y. Deng, G. Li, G. Chen, and X. He, "Evaluation and comparison of the low-frequency oscillation damping methods for the droop-controlled inverters in distributed generation systems," *J. Power Electron.*, vol. 16, no. 2, pp. 731–747, 2016.

[39] S. Li and J. Li, "Output predictor-based active disturbance rejection control for a wind energy conversion system with PMSG," *IEEE Access*, vol. 5, pp. 5205–5214, 2017.

[40] L. Zhang, L. Harnefors, and H.-P. Nee, "Power-synchronization control of grid-connected voltage-source converters," *IEEE Trans. Power Syst.*, vol. 25, no. 2, pp. 809–820, May 2010.

[41] M. G. Taul, X. Wang, P. Davari, and F. Blaabjerg, "Robust fault ride through of converter-based generation during severe faults with phase jumps," *IEEE Trans. Ind. Appl.*, vol. 56, no. 1, pp. 570–583, Jan./Feb. 2020.

[42] X. He, H. Geng, R. Li, and B. C. Pal, "Transient stability analysis and enhancement of renewable energy conversion system during lvrt," *IEEE Trans. Sustain. Energy*, vol. 11, no. 3, pp. 1612–1623, Jul. 2020.

[43] H. Wu and X. Wang, "Transient angle stability analysis of grid-connected converters with the first-order active power loop," in *Proc. 2018 IEEE Appl. Power Electron. Conf. Expo.*, 2018, pp. 3011–3016.

[44] H. Geng, L. Liu, and R. Li, "Synchronization and reactive current support of PMSG-based wind farm during severe grid fault," *IEEE Trans. Sustain. Energy*, vol. 9, no. 4, pp. 1596–1604, Oct. 2018.

[45] D. Pan, X. Wang, F. Liu, and R. Shi, "Transient stability of voltage-source converters with grid-forming control: A design-oriented study," *IEEE Trans. Emerg. Sel. Topics Power Electron.*, vol. 8, no. 2, pp. 1019–1033, Jun. 2020.

[46] H. Wu and X. Wang, "A mode-adaptive power-angle control method for transient stability enhancement of virtual synchronous generators," *IEEE Trans. Emerg. Sel. Topics Power Electron.*, vol. 8, no. 2, pp. 1034–1049, Jun. 2020.

[47] Z. Shuai, C. Shen, X. Liu, Z. Li, and Z. J. Shen, "Transient angle stability of virtual synchronous generators using Lyapunov's direct method," *IEEE Trans. Smart Grid*, vol. 10, no. 4, pp. 4648–4661, Jul. 2019.

[48] D. Pan, X. Wang, F. Liu, and R. Shi, "Transient stability impact of reactive power control on grid-connected converters," in *Proc. IEEE Energy Convers. Congr. Expo.*, 2019, pp. 4311–4316.

[49] J. Wang, Y. Wang, Y. Gu, W. Li, and X. He, "Synchronous frequency resonance of virtual synchronous generators and damping control," in *Proc. 9th Int. Conf. Power Electron. ECCE Asia*, 2015, pp. 1011–1016.

[50] O. Göksu, R. Teodorescu, C. L. Bak, F. Iov, and P. C. Kjær, "Instability of wind turbine converters during current injection to low voltage grid faults and PLL frequency based stability solution," *IEEE Trans. Power Syst.*, vol. 29, no. 4, pp. 1683–1691, Jul. 2014.

[51] M. B. Shadmand, M. Mosa, R. S. Balog, and H. A. Rub, "An improved MPPT technique for high gain DC-DC converter using model predictive control for photovoltaic applications," in *Proc. IEEE Appl. Power Electron. Conf. Expo.*, 2014, pp. 2993–2999.

[52] T. L. Vandoorn, J. D. De Kooning, B. Meersman, and L. Vandevelde, "Review of primary control strategies for islanded microgrids with power-electronic interfaces," *Renewable Sustain. Energy Rev.*, vol. 19, pp. 613–628, 2013.

[53] R. Heydari, M. Gheisarnejad, M. H. Khooban, T. Dragicevic, and F. Blaabjerg, "Robust and fast voltage-source-converter (VSC) control for naval shipboard microgrids," *IEEE Trans. Power Electron.*, vol. 34, no. 9, pp. 8299–8303, Sep. 2019.

[54] T. Dragicevic, "Model predictive control of power converters for robust and fast operation of AC microgrids," *IEEE Trans. Power Electron.*, vol. 33, no. 7, pp. 6304–6317, Jul. 2018.

[55] P. Karamanakos, E. Liegmann, T. Geyer, and R. Kennel, "Model predictive control of power electronic systems: Methods, results, and challenges," *IEEE Open J. Ind. Appl.*, vol. 1, pp. 95–114, 2020.

[56] A. Robey et al., "Learning control barrier functions from expert demonstrations," in *Proc. 2020 59th IEEE Conf. Decis. Control.*, 2020, pp. 3717–3724.

[57] F. Z. Peng and J.-S. Lai, "Generalized instantaneous reactive power theory for three-phase power systems," *IEEE Trans. Instrum. Meas.*, vol. 45, no. 1, pp. 293–297, Feb. 1996.

[58] T. Noguchi, H. Tomiki, S. Kondo, and I. Takahashi, "Direct power control of PWM converter without power-source voltage sensors," *IEEE Trans. Ind. Appl.*, vol. 34, no. 3, pp. 473–479, May/Jun. 1998.

[59] W.-H. Chen, J. Yang, L. Guo, and S. Li, "Disturbance-observer-based control and related methods—an overview," *IEEE Trans. Ind. Electron.*, vol. 63, no. 2, pp. 1083–1095, Feb. 2016.

[60] H. Sira-Ramírez, "From flatness, GPI observers, GPI control and flat filters to observer-based ADRC," *Control Theory Technol.*, vol. 16, no. 4, pp. 249–260, 2018.

[61] S. Li, J. Yang, W.-H. Chen, and X. Chen, *Disturbance Observer-Based Control: Methods and Applications*. Boca Raton, FL, USA: CRC Press, 2014.

[62] H. K. Khalil, *Nonlinear Systems*, 3rd ed. New York, NY, USA: Pearson, 2015.

[63] L. Harnefors, X. Wang, A. G. Yepes, and F. Blaabjerg, "Passivity-based stability assessment of grid-connected VSCs—an overview," *IEEE Trans. Emerg. Sel. Topics Power Electron.*, vol. 4, no. 1, pp. 116–125, Mar. 2016.

[64] P. Karamanakos and T. Geyer, "Guidelines for the design of finite control set model predictive controllers," *IEEE Trans. Power Electron.*, vol. 35, no. 7, pp. 7434–7450, Jul. 2020.

[65] J. Rodriguez and P. Cortes, *Predictive Control of Power Converters and Electrical Drives*, vol. 40. Hoboken, NJ, USA: Wiley, 2012.

[66] M. Novak, V. Ferreira, M. Andresen, T. Dragicevic, F. Blaabjerg, and M. Liserre, "FS-MPC based thermal stress balancing and reliability analysis for npc converters," *IEEE Open J. Power Electron.*, vol. 2, pp. 124–137, 2021.

[67] P. Karamanakos, M. A. Waris Begh, S. Rahmanpour, and T. Geyer, "Gradient-based predictive pulse pattern control for grid-connected converters with LCL filters," in *Proc. 2023 IEEE Energy Convers. Congr. Expo.*, 2023, pp. 2645–2652.

[68] I. Harbi et al., "Model-predictive control of multilevel inverters: Challenges, recent advances, and trends," *IEEE Trans. Power Electron.*, vol. 38, no. 9, pp. 10845–10868, Sep. 2023.

[69] O. Babayomi, Z. Zhang, T. Dragicevic, J. Hu, and J. Rodriguez, "Smart grid evolution: Predictive control of distributed energy resources—A review," *Int. J. Elect. Power Energy Syst.*, vol. 147, 2023, Art. no. 108812.

[70] Z. Zhang et al., "Advances and opportunities in the model predictive control of microgrids: Part I–primary layer," *Int. J. Elect. Power Energy Syst.*, vol. 134, 2022, Art. no. 107411.

[71] J. V. M. Farias, L.-A. Grégoire, A. F. Cupertino, H. A. Pereira, S. I. Seleme, and M. Fadel, "A sliding-mode observer for MMC-HVDC systems: Fault-tolerant scheme with reduced number of sensors," *IEEE Trans. Power Del.*, vol. 38, no. 2, pp. 867–876, Apr. 2023.

[72] J. Liu et al., "Sliding mode control of grid-connected neutral-point-clamped converters via high-gain observer," *IEEE Trans. Ind. Electron.*, vol. 69, no. 4, pp. 4010–4021, Apr. 2022.

[73] L. Liu et al., "A robust high-quality current control with fast convergence for three-level NPC converters in microenergy systems," *IEEE Trans. Ind. Informat.*, vol. 19, no. 11, pp. 10716–10726, Nov. 2023.

[74] N. Altin, S. Ozdemir, H. Komurcugil, and I. Sefa, "Sliding-mode control in natural frame with reduced number of sensors for three-phase grid-tied LCL-interfaced inverters," *IEEE Trans. Ind. Electron.*, vol. 66, no. 4, pp. 2903–2913, Apr. 2019.

[75] B. Long et al., "Passivity fractional-order sliding-mode control of grid-connected converter with LCL filter," *IEEE Trans. Power Electron.*, vol. 38, no. 6, pp. 6969–6982, Jun. 2023.

[76] B. Long, P. J. Lu, K. T. Chong, J. Rodriguez, and J. M. Guerrero, "Robust fuzzy-fractional-order nonsingular terminal sliding-mode control of LCL-type grid-connected converters," *IEEE Trans. Ind. Electron.*, vol. 69, no. 6, pp. 5854–5866, Jun. 2022.

[77] Y. Gui, C. Kim, C. C. Chung, J. M. Guerrero, Y. Guan, and J. C. Vasquez, "Improved direct power control for grid-connected voltage source converters," *IEEE Trans. Ind. Electron.*, vol. 65, no. 10, pp. 8041–8051, Oct. 2018.

[78] Y. Zhang and Z. Min, "Model-free predictive current control of a PWM rectifier based on space vector modulation under unbalanced and distorted grid conditions," *IEEE Trans. Emerg. Sel. Topics Power Electron.*, vol. 10, no. 2, pp. 2319–2329, Apr. 2022.

[79] Y. Zhang, J. Jiao, and J. Liu, "Direct power control of PWM rectifiers with online inductance identification under unbalanced and distorted network conditions," *IEEE Trans. Power Electron.*, vol. 34, no. 12, pp. 12524–12537, Dec. 2019.

[80] M. Ahmed, I. Harbi, R. Kennel, and M. Abdelrahem, "Direct power control based on dead-beat function and extended Kalman filter for PV systems," *J. Modern Power Syst. Clean Energy*, vol. 11, no. 3, pp. 863–872, 2023.

[81] B. Guo, S. Bacha, M. Alamir, A. Hably, and C. Boudinet, "Generalized integrator-extended state observer with applications to grid-connected converters in the presence of disturbances," *IEEE Trans. Control Syst. Technol.*, vol. 29, no. 2, pp. 744–755, Mar. 2021.

[82] T. V. Tran, K.-H. Kim, and J.-S. Lai, "Optimized active disturbance rejection control with resonant extended state observer for grid voltage sensorless LCL-filtered inverter," *IEEE Trans. Power Electron.*, vol. 36, no. 11, pp. 13317–13331, Nov. 2021.

[83] O. Babayomi and Z. Zhang, "Model-free predictive control of power converters with multifrequency extended state observers," *IEEE Trans. Ind. Electron.*, vol. 70, no. 11, pp. 11379–11389, Nov. 2023.

[84] Y. Liu et al., "Passivity-based decoupling control strategy of single-phase LCL-type VSRS for harmonics suppression in railway power systems," *Int. J. Elect. Power Energy Syst.*, vol. 117, 2020, Art. no. 105698.

[85] Y. Gui and Y. Xue, "Passivity-based control of grid forming and grid following converters in microgrids," in *Proc. 2023 IEEE Power Energy Soc. Gen. Meeting*., 2023, pp. 1–5.

[86] L. Harnefors, A. G. Yepes, A. Vidal, and J. Doval-Gandoy, "Passivity-based controller design of grid-connected VSCS for prevention of electrical resonance instability," *IEEE Trans. Ind. Electron.*, vol. 62, no. 2, pp. 702–710, Feb. 2015.

[87] X. Wang, F. Blaabjerg, and P. C. Loh, "Passivity-based stability analysis and damping injection for multiparalleled VSCs with LCL filters," *IEEE Trans. Power Electron.*, vol. 32, no. 11, pp. 8922–8935, Nov. 2017.

[88] C. Xie, K. Li, J. Zou, and J. M. Guerrero, "Passivity-based stabilization of LCL-type grid-connected inverters via a general admittance model," *IEEE Trans. Power Electron.*, vol. 35, no. 6, pp. 6636–6648, Jun. 2020.

[89] Y. Yang et al., "Multiple-voltage-Vector model predictive control with reduced complexity for multilevel inverters," *IEEE Trans. Transport. Electrific.*, vol. 6, no. 1, pp. 105–117, Mar. 2020.

[90] Y. Wang, F. Liu, S. Chen, G. Shen, and Q.-G. Wang, "Prediction errors analysis and correction on FCS-MPC for the cascaded h-bridge multilevel inverter," *IEEE Trans. Ind. Electron.*, vol. 69, no. 8, pp. 8264–8273, Aug. 2022.

[91] O. Babayomi and Z. Zhang, "Model-free predictive control of power converters with cascade-parallel extended state observers," *IEEE Trans. Ind. Electron.*, vol. 70, no. 10, pp. 10215–10226, Oct. 2023.

[92] B. Long et al., "Passivity-based partial sequential model predictive control of t-type grid-connected converters with dynamic damping injection," *IEEE Trans. Power Electron.*, vol. 38, no. 7, pp. 8262–8281, Jul. 2023.

[93] X. Yang, Y. Lyu, K. Wang, U. Kim, Z. Zhang, and K.-B. Park, "A computationally efficient FCS-MPC imitator for grid-tied three-level NPC power converters based on sequential artificial neural network," in *Proc. 2022 IEEE Energy Convers. Congr. Expo.*, 2022, pp. 1–6.

[94] B. Long, T. Cao, W. Fang, K. T. Chong, and J. M. Guerrero, "Model predictive control of a three-phase two-level four-leg grid-connected converter based on sphere decoding method," *IEEE Trans. Power Electron.*, vol. 36, no. 2, pp. 2283–2297, Feb. 2021.

[95] M. Gheisarnejad et al., "Design of ultra-local model control based on interval type-2 fuzzy logic for nine-level packed E-cell," *IEEE J. Emerg. Sel. Topics Ind. Electron.*, vol. 5, no. 1, pp. 72–80, Jan. 2024.

[96] M. Mehrasa, M. Babaie, M. Sharifzadeh, and K. Al-Haddad, "An input–output feedback linearization control method synthesized by artificial neural network for grid-tied packed E-cell inverter," *IEEE Trans. Ind. Appl.*, vol. 57, no. 3, pp. 3131–3142, May/Jun. 2021.

[97] M. Mehrasa, M. Babaie, A. Zafari, and K. Al-Haddad, "Passivity anfis-based control for an intelligent compact multilevel converter," *IEEE Trans. Ind. Informat.*, vol. 17, no. 8, pp. 5141–5151, Aug. 2021.

[98] A. Sepehr, O. Gomis-Bellmunt, and E. Pouresmaeil, "Employing machine learning for enhancing transient stability of power synchronization control during fault conditions in weak grids," *IEEE Trans. Smart Grid*, vol. 13, no. 3, pp. 2121–2131, May 2022.

[99] S. Saadatmand, P. Shamsi, and M. Ferdowsi, "Power and frequency regulation of synchronverters using a model free neural network-based predictive controller," *IEEE Trans. Ind. Electron.*, vol. 68, no. 5, pp. 3662–3671, May 2021.

[100] P. R. Bana and M. Amin, "Control for grid-connected VSC with improved damping based on physics-informed neural network," *IEEE J. Emerg. Sel. Topics Ind. Electron.*, vol. 4, no. 3, pp. 878–888, Jul. 2023.

[101] H. Wang, Q. Huang, and Z. S. Li, "A dynamic bayesian network control strategy for modeling grid-connected inverter stability," *IEEE Trans. Rel.*, vol. 71, no. 1, pp. 75–86, Mar. 2022.

[102] M. M. Mardani, R. D. Lazar, N. Mijatovic, and T. Dragičević, "Artificial neural network-based constrained predictive real-time parameter adaptation controller for grid-tied VSCs," *IEEE Trans. Emerg. Sel. Topics Power Electron.*, vol. 11, no. 2, pp. 1507–1517, Apr. 2023.

[103] L. Liu, Z. Zhang, Y. Yin, S. Vazquez, Y. Zhao, and R. Kennel, "An efficient robust power–voltage control for three-level NPC converters in microgrids," *IEEE Trans. Ind. Informat.*, vol. 20, no. 4, pp. 5849–5863, Apr. 2023.

[104] Q. Xing et al., "Bias-free predictive control of power converters with LCL filter in micro-energy systems," *IEEE Trans. Ind. Electron.*, vol. 70, no. 6, pp. 5907–5916, Jun. 2023.

[105] J. Ma, W. Song, S. Wang, and X. Feng, "Model predictive direct power control for single phase three-level rectifier at low switching frequency," *IEEE Trans. Power Electron.*, vol. 33, no. 2, pp. 1050–1062, Feb. 2018.

[106] O. Babayomi, Z. Zhang, Z. Li, M. L. Heldwein, and J. Rodriguez, "Robust predictive control of grid-connected converters: Sensor noise suppression with parallel-cascade extended state observer," *IEEE Trans. Ind. Electron.*, vol. 71, no. 4, pp. 3728–3740, Apr. 2024.

[107] B. Zhang, "Self-tuning pi controller using pso algorithm to control active and reactive power of VSCs in microgrids," *Int. J. Dyn. Control*, vol. 1, Mar. 2024, Art. no. 15.

[108] M. Easley, S. Jain, M. Shadmand, and H. Abu-Rub, "Autonomous model predictive controlled smart inverter with proactive grid fault ride-through capability," *IEEE Trans. Energy Convers.*, vol. 35, no. 4, pp. 1825–1836, Dec. 2020.

[109] M. J. Morshed and A. Fekih, "A fault-tolerant control paradigm for microgrid-connected wind energy systems," *IEEE Syst. J.*, vol. 12, no. 1, pp. 360–372, Mar. 2018.

[110] M. N. Uddin, M. S. Arifin, and N. Rezaei, "A novel neuro-fuzzy based direct power control of a DFIG based wind farm incorporated with distance protection scheme and LVRT capability," *IEEE Trans. Ind. Appl.*, vol. 59, no. 5, pp. 5792–5803, Sep./Oct. 2023.

[111] P. S. Ghomi, M. Babalou, and H. Torkaman, "Open-circuit fault diagnosis of fault-tolerant DAB converter for improving smart transformers reliability using 1-D CNN," in *Proc. 3rd Int. Conf. Elect. Mach. Drives*, 2023, pp. 1–6.

[112] O. O. Babayomi and P. O. Oluseyi, "Intelligent fault diagnosis in a power distribution network," *Adv. Elect. Eng.*, vol. 2016, 2016, Art. no. 8651630.

[113] M. N. Musarrat, A. Fekih, M. A. Rahman, M. R. Islam, and K. M. Muttaqi, "An event triggered sliding mode control-based fault ride-through scheme to improve the transient stability of wind energy systems," *IEEE Trans. Ind. Appl.*, vol. 60, no. 1, pp. 876–886, Jan./Feb. 2024.

[114] J. Jongudomkarn, J. Liu, and T. Ise, "Virtual synchronous generator control with reliable fault ride-through ability: A solution based on finite-set model predictive control," *IEEE Trans. Emerg. Sel. Topics Power Electron.*, vol. 8, no. 4, pp. 3811–3824, Dec. 2020.

[115] S. R. Mohapatra and V. Agarwal, "Model predictive control for flexible reduction of active power oscillation in grid-tied multilevel inverters under unbalanced and distorted microgrid conditions," *IEEE Trans. Ind. Appl.*, vol. 56, no. 2, pp. 1107–1115, Mar./Apr. 2020.

[116] Y. Yin et al., "Observer-based sliding-mode control for grid-connected power converters under unbalanced grid conditions," *IEEE Trans. Ind. Electron.*, vol. 69, no. 1, pp. 517–527, Jan. 2022.

[117] M. S. Eslahi, S. Vaez-Zadeh, and J. Rodriguez, "Resiliency enhancement and power quality optimization of converter-based renewable energy microgrids," *IEEE Trans. Power Electron.*, vol. 38, no. 6, pp. 7785–7795, Jun. 2023.

[118] X. Xing and H. Chen, "A fast-processing predictive control strategy for common-mode voltage reduction in parallel three-level inverters," *IEEE Trans. Emerg. Sel. Topics Power Electron.*, vol. 9, no. 1, pp. 316–326, Feb. 2021.

[119] T. Liu, A. Chen, and Y. Huang, "Multivector model predictive current control for paralleled three-level t-type inverters with circulating current elimination," *IEEE Trans. Ind. Electron.*, vol. 70, no. 8, pp. 8042–8052, Aug. 2023.

[120] Y. Li, H. He, Z. Li, and Z. Zhang, "Predictive zero-sequence current control of multiple paralleled power converters," *IEEE Trans. Ind. Electron.*, vol. 69, no. 12, pp. 11868–11878, Dec. 2022.

[121] C. Jiang, Z. Quan, D. Zhou, and Y. Li, "A centralized CB-MPC to suppress low-frequency ZSCC in modular parallel converters," *IEEE Trans. Ind. Electron.*, vol. 68, no. 4, pp. 2760–2771, Apr. 2021.

[122] R. Fu, X. Wang, Y. Zhang, and L. Li, "Inertial and primary frequency response of PLL synchronized VSC interfaced energy resources," *IEEE Trans. Power Syst.*, vol. 37, no. 4, pp. 2998–3013, Jul. 2022.

[123] F. Bagheri, H. Komurcugil, and O. Kukrer, "Fixed switching frequency sliding-mode control methodology for single-phase LCL-filtered quasi-z-source grid-tied inverters," in *Proc. IEEE 12th Int. Conf. Compat., Power Electron. Power Eng.*, 2018, pp. 1–6.

[124] Y. Zhang, J. Jiao, and D. Xu, "Direct power control of doubly fed induction generator using extended power theory under unbalanced network," *IEEE Trans. Power Electron.*, vol. 34, no. 12, pp. 12024–12037, Dec. 2019.

[125] X. Shen et al., "High-performance second-order sliding mode control for NPC converters," *IEEE Trans. Ind. Inform.*, vol. 16, no. 8, pp. 5345–5356, Aug. 2020.

[126] X. Shen et al., "Adaptive second-order sliding mode control for grid-connected NPC converters with enhanced disturbance rejection," *IEEE Trans. Power Electron.*, vol. 37, no. 1, pp. 206–220, Jan. 2022.

[127] H. Komurcugil, S. Biricik, S. Bayhan, and Z. Zhang, "Sliding mode control: Overview of its applications in power converters," *IEEE Ind. Electron. Mag.*, vol. 15, no. 1, pp. 40–49, Mar. 2021.

[128] M. P. Kazmierkowski, M. Jasinski, and G. Wrona, "DSP-based control of grid-connected power converters operating under grid distortions," *IEEE Trans. Ind. Informat.*, vol. 7, no. 2, pp. 204–211, May 2011.

[129] J. Hu, L. Shang, Y. He, and Z. Q. Zhu, "Direct active and reactive power regulation of grid-connected dc/ac converters using sliding mode control approach," *IEEE Trans. Power Electron.*, vol. 26, no. 1, pp. 210–222, Jan. 2011.

[130] Y. Zhang, W. Xie, Z. Li, and Y. Zhang, "Model predictive direct power control of a PWM rectifier with duty cycle optimization," *IEEE Trans. Power Electron.*, vol. 28, no. 11, pp. 5343–5351, Nov. 2013.

[131] Y. Sun, Z. Zhang, Y. Wang, Z. Li, and J. Rodriguez, "Robust predictive control of grid-tied modular multilevel converters for HVDC systems with virtual-flux based online inductance estimation," *IEEE Trans. Power Del.*, vol. 37, no. 4, pp. 3189–3199, Aug. 2022.

[132] M. Malinowski, M. Jasinski, and M. Kazmierkowski, "Simple direct power control of three-phase PWM rectifier using space-vector modulation (DPC-SVM)," *IEEE Trans. Ind. Electron.*, vol. 51, no. 2, pp. 447–454, Apr. 2004.

[133] M. Malinowski, M. Kazmierkowski, S. Hansen, F. Blaabjerg, and G. Marques, "Virtual-flux-based direct power control of three-phase pwm rectifiers," *IEEE Trans. Ind. Appl.*, vol. 37, no. 4, pp. 1019–1027, Jul./Aug. 2001.

[134] A. Benrabah, D. Xu, and Z. Gao, "Active disturbance rejection control of LCL-filtered grid-connected inverter using padé approximation," *IEEE Trans. Ind. Appl.*, vol. 54, no. 6, pp. 6179–6189, Nov./Dec. 2018.

[135] Y. Cao, Q. Zhao, Y. Ye, and Y. Xiong, "ADRC-based current control for grid-tied inverters: Design, analysis, and verification," *IEEE Trans. Ind. Electron.*, vol. 67, no. 10, pp. 8428–8437, Oct. 2020.

[136] C. Cheng, S. Xie, Q. Qian, J. Lv, and J. Xu, "Observer-based single-sensor control schemes for LCL-filtered grid-following inverters," *IEEE Trans. Ind. Electron.*, vol. 70, no. 5, pp. 4887–4900, May 2023.

[137] J. Zhao, C. Xie, K. Li, J. Zou, and J. M. Guerrero, "Passivity-oriented design of LCL-type grid-connected inverters with Luenberger observer-based active damping," *IEEE Trans. Power Electron.*, vol. 37, no. 3, pp. 2625–2635, Mar. 2022.

[138] M. Bouzidi, S. Barkat, A. Krama, and H. Abu-Rub, "Generalized predictive direct power control with constant switching frequency for multilevel four-leg grid connected converter," *IEEE Trans. Power Electron.*, vol. 37, no. 6, pp. 6625–6636, Jun. 2022.

[139] P. R. U. Guazzelli, W. C. de Andrade Pereira, C. M. R. de Oliveira, A. G. de Castro, and M. L. de Aguiar, "Weighting factors optimization of predictive torque control of induction motor by multiobjective genetic algorithm," *IEEE Trans. Power Electron.*, vol. 34, no. 7, pp. 6628–6638, Jul. 2019.

[140] M. Babaie, M. Mehrasa, M. Sharifzadeh, and K. Al-Haddad, "Floating weighting factors ANN-MPC Based on Lyapunov stability for seven-level modified PUC active rectifier," *IEEE Trans. Ind. Electron.*, vol. 69, no. 1, pp. 387–398, Jan. 2022.

[141] J. Wang, X. Liu, Q. Xiao, D. Zhou, H. Qiu, and Y. Tang, "Modulated model predictive control for modular multilevel converters with easy implementation and enhanced steady-state performance," *IEEE Trans. Power Electron.*, vol. 35, no. 9, pp. 9107–9118, Sep. 2020.

[142] R. Heydari et al., "Model-free predictive control of grid-forming inverters with LCL filters," *IEEE Trans. Power Electron.*, vol. 37, no. 8, pp. 9200–9211, Aug. 2022.

[143] H. Chen, Z. Zhang, Z. Li, P. Zhang, and M. Zhang, "Data-driven predictive current control for active front ends with neural networks," in *Proc. IEEE 17th Conf. Ind. Electron. Appl.*, 2022, pp. 201–206.

[144] R. O. Ramírez, C. R. Baier, F. Villarroel, J. R. Espinoza, J. Pou, and J. Rodríguez, "A hybrid FCS-MPC with low and fixed switching frequency without steady-state error applied to a grid-connected CHB inverter," *IEEE Access*, vol. 8, pp. 223637–223651, 2020.

[145] H. Mahmoudi, M. Aleenejad, and R. Ahmadi, "Modulated model predictive control of modular multilevel converters in VSC-HVDC systems," *IEEE Trans. Power Del.*, vol. 33, no. 5, pp. 2115–2124, Oct. 2018.

[146] D. Schuetz et al., "Space vector modulated model predictive control for grid-tied converters," *IEEE Trans. Ind. Inform.*, vol. 19, no. 1, pp. 414–425, Jan. 2023.

[147] A. Mora et al., "Predictive optimal switching sequence direct power control for grid-tied 3l-NPC converters," *IEEE Trans. Ind. Electron.*, vol. 68, no. 9, pp. 8561–8571, Sep. 2021.

[148] A. Kaymanesh, A. Chandra, and K. Al-Haddad, "Model predictive control of MPUC7-Based STATCOM using autotuned weighting factors," *IEEE Trans. Ind. Electron.*, vol. 69, no. 3, pp. 2447–2458, Mar. 2022.

[149] O. Babayomi, Z. Zhang, Y. Li, and R. Kennel, "Adaptive predictive control with neuro-fuzzy parameter estimation for microgrid grid-forming converters," *Sustainability*, vol. 13, no. 13, 2021, Art. no. 7038.

[150] M. Fliess and C. Join, "Model-free control," *Int. J. Control*, vol. 86, no. 12, pp. 2228–2252, Dec. 2013.

[151] T. Zhao, M. Zhang, C. Wang, and Q. Sun, "Model-free predictive current control of three-level grid-connected inverters with LCL filters based on kalman filter," *IEEE Access*, vol. 11, pp. 21631–21640, 2023.

[152] B. Long, J. Zhang, D. Shen, J. Rodríguez, J. M. Guerrero, and K. T. Chong, "Ultralocal model-free predictive control of t-type grid-connected converters based on extended sliding-mode disturbance observer," *IEEE Trans. Power Electron.*, vol. 38, no. 12, pp. 15494–15508, Dec. 2023.

[153] R. Baidya, R. P. Aguilera, P. Acuña, S. Vazquez, and H. d. T. Mouton, "Multistep model predictive control for cascaded h-bridge inverters: Formulation and analysis," *IEEE Trans. Power Electron.*, vol. 33, no. 1, pp. 876–886, Jan. 2018.

[154] D. E. Quevedo, R. P. Aguilera, and T. Geyer, "Predictive control in power electronics and drives: Basic concepts, theory, and methods," *Adv. Intell. Control Power Electron. Drives*, pp. 181–226, 2014.

[155] X. Fu and S. Li, "Control of single-phase grid-connected converters with LCL filters using recurrent neural network and conventional control methods," *IEEE Trans. Power Electron.*, vol. 31, no. 7, pp. 5354–5364, Jul. 2016.

[156] Y. Sun, S. Li, B. Lin, X. Fu, M. Ramezani, and I. Jaithwa, "Artificial neural network for control and grid integration of residential solar photovoltaic systems," *IEEE Trans. Sustain. Energy*, vol. 8, no. 4, pp. 1484–1495, Oct. 2017.

[157] S. Sahoo and F. Blaabjerg, "Data-driven controllability of power electronics under boundary conditions - a physics-informed neural network based approach," in *Proc. 2023 IEEE Appl. Power Electron. Conf. Expo.*, 2023, pp. 2801–2806.

[158] K. Zeb et al., "High-performance and multi-functional control of transformerless single-phase smart inverter for grid-connected PV system," *J. Modern Power Syst. Clean Energy*, vol. 9, no. 6, pp. 1386–1394, 2021.

[159] M. Gheisarnejad, M. Sharifzadeh, M.-H. Khooban, and K. Al-Haddad, "Adaptive fuzzy Q-learning control design and application to grid-tied nine-level packed E-cell (PEC9) inverter," *IEEE Trans. Ind. Electron.*, vol. 70, no. 1, pp. 1071–1076, Jan. 2023.

[160] M. Babaie and K. Al-Haddad, "Self-training intelligent predictive control for grid-tied transformerless multilevel converters," *IEEE Trans. Power Electron.*, vol. 38, no. 10, pp. 12482–12496, Oct. 2023.

[161] Y. Zhu and J. Fei, "Disturbance observer based fuzzy sliding mode control of PV grid connected inverter," *IEEE Access*, vol. 6, pp. 21202–21211, 2018.

[162] Y. Mi, Y. Song, Y. Fu, and C. Wang, "The adaptive sliding mode reactive power control strategy for wind–diesel power system based on sliding mode observer," *IEEE Trans. Sustain. Energy*, vol. 11, no. 4, pp. 2241–2251, Oct. 2020.

[163] S. Wang, T. Dragicevic, Y. Gao, and R. Teodorescu, "Neural network based model predictive controllers for modular multilevel converters," *IEEE Trans. Energy Convers.*, vol. 36, no. 2, pp. 1562–1571, Jun. 2021.

[164] S. A. Zaid et al., "From MPC-based to end-to-end (E2E) learning-based control policy for grid-tied 3l-NPC transformerless inverter," *IEEE Access*, vol. 10, pp. 57309–57326, 2022.

[165] P. R. Bana, M. Amin, and M. Molinas, "Ann-based surrogate pi and MPC controllers for grid-connected VSC system: Small-signal analysis and comparative evaluation," *IEEE J. Emerg. Sel. Top. Power Electron.*, vol. 12, no. 1, pp. 566–578, Feb. 2024.

[166] M. Zhang, Y. Zhang, and Q. Xu, "Transfer learning based online impedance identification for modular multilevel converters," *IEEE Trans. Power Electron.*, vol. 38, no. 10, pp. 12207–12218, Oct. 2023.

[167] A. Adib, B. Mirafzal, X. Wang, and F. Blaabjerg, "On stability of voltage source inverters in weak grids," *IEEE Access*, vol. 6, pp. 4427–4439, 2018.

[168] R. Wu, F. Blaabjerg, H. Wang, M. Liserre, and F. Iannuzzo, "Catastrophic failure and fault-tolerant design of IGBT power electronic converters - An overview," in *Proc. IECON 2013-39th Annu. Conf. IEEE Ind. Electron. Soc.*, 2013, pp. 507–513.

[169] T. Dragičević, P. Wheeler, and F. Blaabjerg, "Artificial intelligence aided automated design for reliability of power electronic systems," *IEEE Trans. Power Electron.*, vol. 34, no. 8, pp. 7161–7171, Aug. 2019.

[170] Y. Fassi, V. Heiries, J. Boutet, and S. Boisseau, "Toward physics-informed machine-learning-based predictive maintenance for power converters—A review," *IEEE Trans. Power Electron.*, vol. 39, no. 2, pp. 2692–2720, Feb. 2024.

[171] S. Sahoo, T. Dragičević, and F. Blaabjerg, "Cyber security in control of grid-tied power electronic converters—challenges and vulnerabilities," *IEEE Trans. Emerg. Sel. Topics Power Electron.*, vol. 9, no. 5, pp. 5326–5340, Oct. 2021.

[172] T. V. Vu, B. L. Nguyen, Z. Cheng, M.-Y. Chow, and B. Zhang, "Cyber-physical microgrids: Toward future resilient communities," *IEEE Ind. Electron. Mag.*, vol. 14, no. 3, pp. 4–17, Sep. 2020.
[173] W.-H. Ko et al., "Robust dynamic watermarking for cyber-physical security of inverter-based resources in power distribution systems," *IEEE Trans. Ind. Electron.*, vol. 71, no. 7, pp. 7106–7116, Jul. 2024.
[174] X. Wang et al., "A novel model predictive control strategy to eliminate zero-sequence circulating current in paralleled three-level inverters," *IEEE Trans. Emerg. Sel. Topics Power Electron.*, vol. 7, no. 1, pp. 309–320, Mar. 2019.

Oluleke Babayomi (Senior Member, IEEE) received the B.Sc. (Hons) and M.Sc. degrees in electrical and electronics engineering from the University of Lagos, Akoka, Nigeria, in 2006 and 2016, respectively, and the Ph.D. degree in electrical engineering from Shandong University, Jinan, China, in 2023.

Until 2019, he was a Principal Engineer and Software Development Team Lead with the National Space Research and Development Agency, Nigeria. He is currently a Postdoctoral Researcher with the Korea Advanced Institute of Science and Technology, Daejeon, South Korea. His research interests include model predictive control, power electronics, microgrids, and sustainable energy policy.

Dr. Babayomi was the recipient of the 2024 IEEE-PELS Ph.D. Thesis Talk Award. He is the Chair of the IEEE Smart Village Marketing Committee.

Yu Li (Member, IEEE) was born in Shandong, China, in 1986. He received the M.S. degree in power electronics and electric drives from the School of Automation, Northwestern Polytechnical University, Xi'an, China, in 2012, and the Ph.D. degree in electrical engineering from the School of Electrical Engineering, Shandong University, Jinan, China, in 2022.

From 2013 to 2015, he was a Research Engineer with the Department of Electrical and Computer Engineering, Kettering University, Flint, MI, USA. Since 2022, he has been an Assistant Professor with the Laser Institute, Qilu University of Technology (Shandong Academy of Sciences), Jinan, China. His research interests include control in power electronics converters, energy storage systems, and microgrids.

Zhenbin Zhang (Senior Member, IEEE) received the Ph.D. (*summa cum laude*) degree in electrical and energy engineering from the Technical University of Munich, Munich, Germany, in 2016.

He was a Postdoctoral Researcher of electrical and energy engineering with the Technical University of Munich. Since 2017, he has been a Full Professor with Shandong University, Jinan, China, where he is currently the Director for both the Laboratory of More Power Electronics Energy Systems and the Institute of Sustainable Energy and Smart Grids. His research interests include power electronics and electrical drives, sustainable energy systems, smart grids, and microgrids.

Dr. Zhang was the recipient of the VDE Award 2017, Germany. He is an Associate Editor for IEEE TRANSACTIONS POWER ELECTRONICS. He is a Fellow and Chartered Engineer of the Institution of Engineering and Technology.

Ki-Bum Park (Member, IEEE) received the B.S., M.S., and Ph.D. degrees in electrical engineering from Korea Advanced Institute of Science and Technology (KAIST), Daejeon, South Korea, in 2003, 2005, and 2010, respectively.

After nine years of industry experience with ABB Corporate Research, Baden-Daettwil, Switzerland, he is currently with KAIST, as an Associate Professor. His research interests include power conversion system for transportation electrification and renewable integration in association with systemlevel optimization of power electronics.